OPTIMIZATION OF DESIGN PARAMETERS FOR TONPILZ TYPE TRANSDUCERS

A THESIS SUBMITTED TO
THE GRADUATE SCHOOL OF NATURAL AND APPLIED SCIENCES
OF
MIDDLE EAST TECHNICAL UNIVERSITY

BY
MERVE ÇİÇEK

IN PARTIAL FULFILLMENT OF THE REQUIREMENTS
FOR
THE DEGREE OF MASTER OF SCIENCE
IN
MECHANICAL ENGINEERING

DECEMBER, 2014

Approval of the thesis

OPTIMIZATION OF DESIGN PARAMETERS FOR TONPILZ TYPE TRANSDUCERS

submitted by **MERVE ÇİÇEK** in partial fulfillment of the requirement for the degree of **Master of Science in Mechanical Engineering Department, Middle East Technical University** by,

Prof. Dr. Gülbin Dural Ünver _____
Dean of Graduate School of **Natural and Applied Sciences**

Prof. Dr. Tuna Balkan _____
Head of Department, **Mechanical Engineering**

Prof. Dr. Mehmet Çalışkan _____
Supervisor, **Mechanical Engineering Department**

Examining Committee Members

Prof. Dr. Y. Samim Ünlüsoy _____
Mechanical Engineering Department, METU

Prof. Dr. Mehmet Çalışkan _____
Mechanical Engineering Department, METU

Assist. Prof. Dr. Yiğit Yazıcıoğlu _____
Mechanical Engineering Department, METU

Assist. Prof. Dr. Kıvanç Azgın _____
Mechanical Engineering Department, METU

Assoc. Prof. Dr. Barış Bayram _____
Electrical and Electronics Engineering Department, METU

Date: 08/12/2014

I hereby declare that all information in this document has been obtained and presented in accordance with academic rules and ethical conduct. I also declare that, as required by these rules and conduct, I have fully cited and referenced all material and results that are not original to this work.

Name, Last Name: Merve Çiçek

Signature:

ABSTRACT

OPTIMIZATION OF DESIGN PARAMETER FOR TONPILZ TYPE TRANSDUCERS

Çiçek, Merve

M. Sc., Department of Mechanical Engineering

Supervisor: Prof. Dr. Mehmet Çalışkan

December 2014, 81 pages

Design of a Tonpilz type transducer is a complex process involving many design parameters which may affect each other. Therefore, an optimum design is a difficult task to reach. The purpose of this study is to optimize design parameters of Tonpilz type transducers. The study involves three different transducer modeling techniques. Each of these models is explained and benchmarked with the help of published experimental data. The simplest model is exploited to produce initial data for unknown design parameters. Optimization of design parameters are performed with the other two models. Results regarding to the design parameters before and after optimization process are compared. A design parameter set which satisfies the design requirements with maximum output power is obtained by the Finite Element Method.

Keywords: Tonpilz, underwater acoustics, optimization, transducer design, finite element method.

ÖZ

TONPİLZ TİPİ AKUSTİK ÇEVİRİCİLER İÇİN TASARIM PARAMETRELERİ ENİYİLEMESİ

Çiçek, Merve

Yüksek Lisans, Makine Mühendisliği Bölümü

Tez Yöneticisi: Prof. Dr. Mehmet Çalışkan

Aralık 2014, 81 sayfa

Tonpilz tipi akustik çeviricilerin tasarımı birçok birbirini etkileyen tasarım parametresi içeren kompleks bir süreçtir. Bu nedenle, istekleri karşılayan optimum bir sonuç bulmak zor olmaktadır. Bu sorunu çözebilmek için tasarım parametrelerinin eniyilemesinin yapılması gerekmektedir. Bu çalışmada, Tonpilz tipi akustik çeviriciler için tasarım parametreleri eniyilenmiştir. Çalışmada 3 model kullanılmıştır. Kullanılan modellerin ayrıntıları çalışma içerisinde anlatılmıştır. Çalışma içerisinde yer alan modellerden bir tanesi ilk tasarım parametrelerinin elde edilmesi için kullanılmıştır. Eniyileme diğer iki model kullanılarak yapılmıştır. Eniyileme sonucunda elde edilen tasarım parametreleri ve önceki tasarım parametrelerinin karşılaştırma yapılmıştır. Tasarım gereklerini sağlayan ve çıkış gücünü en çoklayan bir tasarım parametre seti sonlu elemanlar metodu ile eniyileme yapılarak bulunmuştur.

Anahtar Kelimeler: Tonpilz, su altı akustiği, eniyileme, akustik çevirici tasarımı, sonlu elemanlar metodu

To Mom, Dad and My Dear Husband

ACKNOWLEDGEMENTS

First of all, I would like to express my sincere gratitude and appreciation to my supervisor Prof. Dr. Mehmet Çalışkan for his invaluable guidance, patience and help throughout the study.

I am also grateful to my company ASELSAN Inc. and my colleagues. I would especially like to state my thanks to Kerim Çepni, Niyazi Şenlik and Umut Batu for their help and assistance.

I would like to give my special thanks to my friends Ayşe Gözde Ulu Soysal, Özge Mencek and Mine Azgın for their encouragement and help whenever needed.

My deepest thanks go to my parents, my brother and his wife: Hatice and Mustafa Soyarslan, Mehmet and Ayşe Sercan Soyarslan for their endless support, patience and love throughout my life. Without them, I would not be able to finish this study.

Last but not least, I am very thankful to my dear husband Kerem Furkan Çiçek. I owe him too much for his encouragement, love and support.

TABLE OF CONTENTS

LIST OF TABLES

LIST OF FIGURES

LIST OF SYMBOLS

Δf	Bandwidth, 1/s
η_{ma}	Electromechanical efficiency
κ_{th}	Tail-to-head mass ratio
ρc	Specific acoustic impedance
ρ_h	Density of head mass, kg/m^3
ρ_t	Density of tail mass, kg/m^3
$tan\delta$	Loss tangent
υ	Poison's ratio
A_h	Area of active surface, m^2
A_{pzt}	Area of piezoceramics, m^2
c	Speed of sound, m/s
C_0	Clamped capacitance
C_f	Free capacitance
D_f	Directivity factor
DI	Directivity index
E_{pzt}	Elastic modulus of piezoceramics,
F_e	Excitation force, N
f_{flex}	Flexural resonance, Hz
f_n	Natural frequency, Hz
K_e	Effective stiffness, N/m
K_g	Stiffness of glue, N/m
K_{pzt}	Stiffness of piezoceramic stack, N/m
l_{pzt}	Length of piezoceramic stack, m
l_t	Length of tail mass, m
M_e	Effective mass, kg
M_h	Mass of the head mass, kg
M_{pzt}	Mass of piezoceramic stack, kg

M_t	Mass of the tail mass, kg
N	Transduction coefficient, N/V
n	Number of piezoceramic rings
Q_m	Mechanical quality factor
R_0	Internal electrical resistance
R_e	Effective damper, Ns/m
R_h	Radiation resistance, Ns/m
R_m	Internal mechanical resistance
r_h	Radius of active surface, m
r_{pzt}	Mean radius of piezoceramic stack, m
r_t	Radius of tail mass, m
SL	Source level, dB
t_h	Thickness of head mass, m
TVR	Transmitting voltage response
V_{drive}	Driving voltage, V
W_e	Input electrical power
ω_n	Angular resonance frequency, rad/s

CHAPTER 1

INTRODUCTION

Sea water shows different characteristics than air in terms of propagation of electromagnetic waves since it is much denser than air and electrically conductive. Therefore, electromagnetic waves cannot be used in water for communication purposes as in air. However, acoustic waves exhibit negligible amount of attenuation in water can propagate over large distances. Thus, acoustic waves dominate almost all underwater applications.

The word SONAR is an acronym of "SOund Navigation And Ranging" which is used for underwater navigation, detection and communication technologies. There exist two types of sonar, namely, active and passive sonar. Active sonar emits signals and listens to echoes to detect and navigate objects while passive sonar just listens to sound under the surface of water. Both active and passive sonar systems use transducers to detect and navigate objects.

Transducer in general is a name given for all devices that convert energy from one form into another. In sonar applications, transducers are used to convert electrical energy into acoustical energy or vice versa. Also transducers can be grouped into two classes according to their usage: projectors and hydrophones. Projectors are used to emit signals to acoustic environment; whereas, hydrophones listen to sound and convert acoustical signals into electrical signals. In this manner, it can be grossly said that hydrophones are underwater microphones. However, some transducers could be used as projectors as well as hydrophones.

Transducers could also be classified according to their transduction mechanisms: piezoelectric transducers, electrostrictive transducers, magnetostrictive transducers,

electrostatic transducers, variable reluctance transducers and moving coil transducers.

Transducers may vary both in size and shape due to their transduction mechanism and application requirements such as frequency, bandwidth, beam width and source level. In this study, design parameters of Tonpilz-type transducers are going to be optimized in order to achieve maximum source level at desired resonance frequency.

The organization of material in this thesis is as follows: In the first chapter, definitions of some basic concepts will be explained for better understanding of subject matter in the following chapters.

The second chapter, a literature survey regarding to transducer models and optimization of transducer design is presented. The third chapter describes different modeling techniques used both in design and optimization processes.

All the models introduced in the third chapter are validated in the fourth chapter with the help of a Tonpilz transducer produced and tested available in the literature. The optimization procedure and optimization results, comparison of design before and after the optimization process are presented in the fifth chapter

The last chapter summarizes the study along with conclusions. Also all the results and future work are discussed in this chapter.

1.1 A Review to History of Underwater Acoustics

Audibility of sound in water is first pointed by Aristotle [1, 25]. The physical understanding of acoustics was advanced by Marin Mersenne and Galileo independently with the discovery of the laws of the vibrating strings. Mersenne measured the speed of sound in air and this study was published *L'Harmonie Universelle* in 1620's. A deeper approach came from Lord Rayleigh (John William Strut). He described the sound waves mathematically and defined the wave equation in his book *Theory of Sound* [2].

The first study about theory of sound was from Sir Isaac Newton, in 1687 with his work namely, *Mathematical Principles of Natural Philosophy.* Even focus of Newton was limited to sound in air, the same mathematical formulas and principles are valid for underwater acoustics [1].

The speed of sound in water was found in an experiment conducted by a Swiss scientist, Daniel Colladon and a French mathematician, Charles Sturm in Lake Geneva, Switzerland in September 1826 [1, 2, 25].

Discovery of transduction mechanisms had great impact on development of underwater acoustics. One of these mechanisms is the magnetostriction discovered by James Joule based on his experiments indicating change in dimension of magnetic material under magnetic field [5]. A leading invention for the development of underwater acoustics is the discovery of piezoelectricity by Jacques and Pierre Curie brothers in 1880 [4, 11].

Discovery of piezoelectricity led transducer technology. Piezoelectric materials can generate sound waves by expanding and contracting when a changing voltage is applied. In 1917, French scientist Paul Langevin became the first person to use piezoelectricity to build echo-ranging system (Figure 1).

Improvement in transducer technology became possible by inventions in material science. World War II and the following years motivated the search for different transduction materials.

Beginning with World War II, advances in electronics such as amplifying and processing of sonar information as well as better understanding of underwater acoustics concepts influenced the developments in underwater acoustics technology for both military and nonmilitary use. The knowledge and developments gained in those days still lead the underwater acoustic technology.

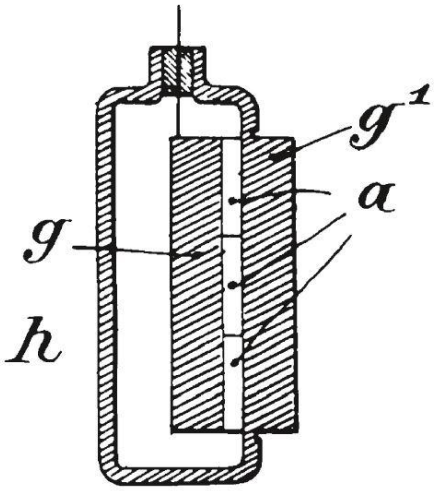

Figure 1: British Patent 145,691, July 28, 1921 of P. Langevin Invention Showing Steel(g)-Quarts(a)-Steel(g') Sandwich Transducer [4]

1.2. Piezoelectricity

The transducer technology had a great improvement when the concept of piezoelectricity was first discovered by Curie brothers in 1880. The original discovery is that an applied pressure could generate electrical voltage for certain crystalline structure materials and known as the piezoelectric effect. The converse effect which is the change in the mechanical strain due to applied electric field is described as the converse/indirect piezoelectric effect.

The reason behind that the piezoelectric ceramics are the most widely used transduction mechanism for the transducer technology is being linear and reciprocal. Application of an electric field causes expansion of the material in the direction of electric field. However, opposing the direction of the electric field ends up with a shrink in dimension.

Beyond these advantages, there are also some drawbacks of piezoceramics. One of these drawbacks is brittleness of piezoceramics. Although being very strong in

compression, they are weak in tension. In addition, they show unpredictable behavior under tension since their tensile strength can vary substantially [8]. Thus, during design procedure, it is crucial that tensile stress should be avoided.

Piezoceramics are formed of crystallites which are sintered at high temperatures, near Curie temperature, and polarized by applying a high electric field [4]. Application of high polarization field results in a permanent polarization, which is very stable, gives a strong piezoelectric effect. However, depolarization can occur at operating temperatures near Curie temperature. This is also an issue that has to be taken into consideration during the design process.

Since the piezoelectric effect is linear, its mathematical representation is formed of a set of linear equations. These equations relate stress, T; strain, S; electric displacement, D; and electric field, E. The corresponding equations are presented in detail in various sources [4, 8, 9].

1.3. General Information about Tonpilz type Transducers

Tonpilz-type transducers were first invented in 1959 as an improvement of their ancestors. Tonpilz, a German word with meaning *"sound mushroom"* was given as name due to mushroom-like shape of these kinds of transducers [4]. As a result of their good performance, simplicity and low cost, they had widespread use area since they have been invented. Another advantage of Tonpilz-type transducers is their property of being useable for wide frequency ranges with variation of dimensions.

Tonpilz-type transducers consist of 33-mode driven piezoceramic stack squeezed with a head mass and a tail mass with the help of a stud and a nut [4] as seen from Figure 2. By means of this configuration, a longitudinal resonance frequency between 1 – 70 kHz could be obtained and long piezoceramic stack is not necessarily required [10]. In most mechanical designs, the resonance frequency is tried to be avoided since the largest displacements occur at resonance frequencies.

In contrast, it is the goal of transducer designing to achieve the resonance frequency because the higher displacement leads higher sound pressure levels transferred to acoustic medium.

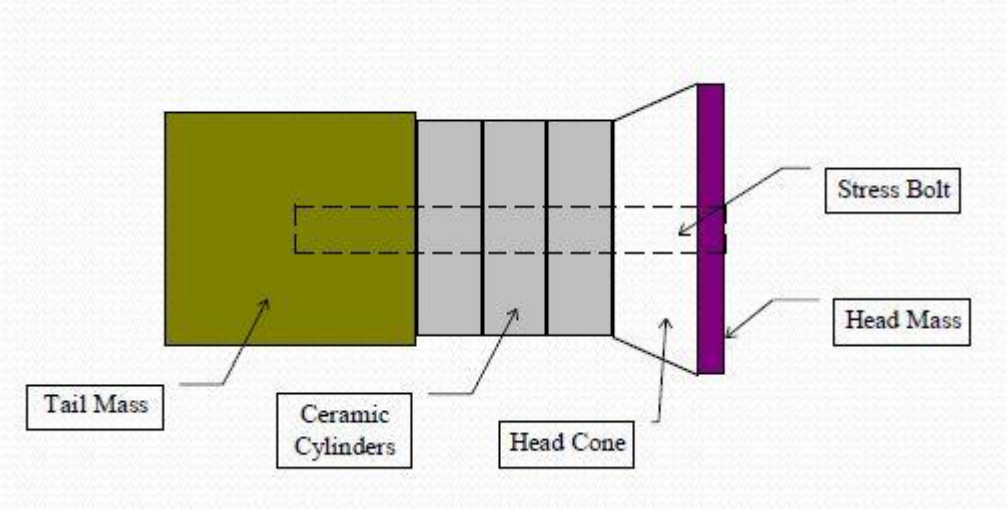

Figure 2: A Representative Sketch for Tonpilz Type Transducers

The piezoceramic stack is responsible for the generation of motion. The acoustical power transferred to acoustic medium is directly related with the response of the ceramic stack. With the applied alternating voltage, mechanically in-series and electrically in-parallel ceramic cylinders expand and contract and generate a pressure perturbation, in other words, sound.

The head mass has a critical importance in transducer design. The surface of the head mass is the place where energy is transferred to the acoustic medium. Thus, it is called the active surface. The shape of the active surface varies according to operational purposes. Circle shape is very common but not very useful for array applications. Instead square-shaped or hexagon-shaped is preferred. In order to maximize the acoustic power, the area of the active surface should be maximized while the head mass is minimized. However such a combination leads a dilution of

the thickness of the head mass which results in a decrease in flexural resonance. Flexural resonance must be avoided since it causes irregular fluctuation of water and null response. Thus, an optimum solution is needed such that both flexural resonance is prevented and acoustical power is enhanced as much as possible.

The other important issue about transducer design is stud and nut system which keeps the head mass, the tail mass and the piezoceramic stack together. Since piezoceramics show unreliable behavior under tensile stress, they should always work under compressive stress even at the expansion mode. A compressive stress higher than the maximum stress encountered due to applied alternating voltage could be attained to prevent tensile stresses. In addition, the stiffness of the stud is significant in design procedure. Higher stiffness means lower energy that transferred to acoustic medium. Besides, the stud is exposed to high frequency alternating stress which may cause fatigue. The material selection is carefully handled to find a stud material which satisfies not much high stiffness and avoids fatigue.

Although tail mass does not have much importance compared to other transducer parts, it affects the resonance frequency of the transducer. To increase the acoustical power as well as bandwidth, the tail mass is required to be as heavy as possible. Nonetheless, increase in total weight of the transducers is not desired generally. Therefore, the mass of the tail mass should be decided meticulously.

Beyond these primary parts of the transducer, there are many other parts which are required for practical use of the transducers (Figure 3).The function these parts is mostly to protect the transducer against water, physical damage and shock, etc. A thin metal housing is generally preferred to preserve the transducer from physical damage. The housing isolates every part of the transducer from water except the head mass. The head mass is protected with pressure relief isolation materials in order not to cause a change in performance of the transducer. Even such materials may affect resonance frequency and acoustical energy transferred to the water, but

this effect can be minimized with the proper material selection. Therefore, design of protective parts is not included in the content of this study.

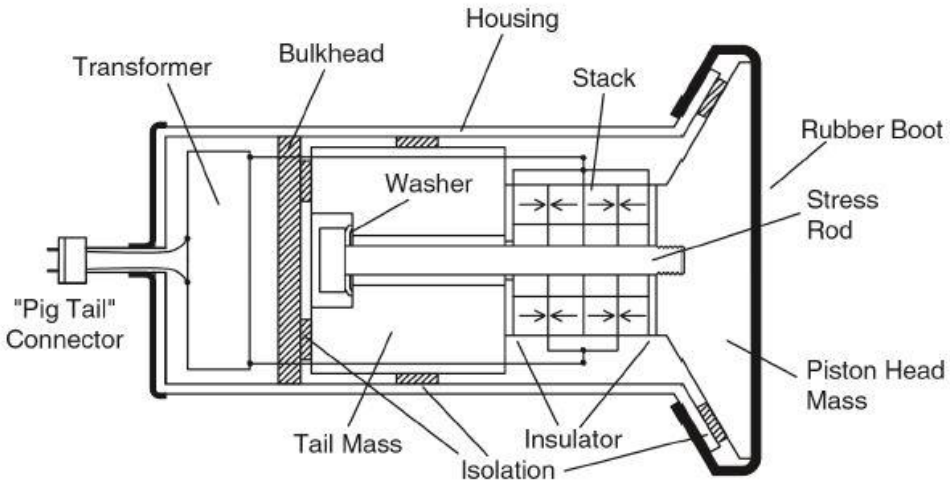

Figure 3: A Detailed Cross-sectional View of Tonpilz-type Transducers

1.4. Basics of Transducers

In order to describe a transducer's characteristics and performance, there exist some concepts used. The fundamental property for identifying a transducer is the resonance, in other words, central frequency. The most reliable way to measure the resonance frequency of a transducer is conductance response. The frequency at which the conductance reaches a peak value is the resonance frequency of the transducer. Conductance can be defined as follows by means of Ohm's Law:

$$Z = \frac{V}{I} \tag{1.1}$$

$$Y = \frac{1}{Z} = G + iB \tag{1.2}$$

where I is the current, V is the voltage, Z is the impedance, Y is the admittance, G is the conductance and B is the susceptance.

Directivity factor and directivity index are also commonly used design parameters. Acoustic axis is the direction in which the acoustic response of the transducer has the maximum value [8]. It is usually at the center of the active surface of Tonpilz-type transducers and normal to the active surface. Then, the directivity factor is defined as the ratio of the transmitted acoustic intensity along acoustic axis (I_0), to the intensity which would have resulted from radiating the same power uniformly in all directions (I_{ref}), both measured at the same distance [8]. Directivity index is just the dB-scale representation of the directivity factor. For Tonpilz-type transducers with a circular active surface, the directivity factor could be calculated as follows [9]

$$D_f = \frac{(ka)^2}{[1 - J_1(2ka)/ka]} \tag{1.3}$$

where k is the wavenumber and a is the radius of the active surface. Then the directivity index is

$$DI = 10\log(D_f) \tag{1.4}$$

In order to express performance of a transducer, two fundamental concepts are commonly used in conjunction. These are namely, transmitting voltage response, TVR, and source level, SL. Both terms represent the intensity at a point 1m away from the active surface of the transducer on the acoustic axis relative to the intensity of an ideal plane wave with a 1μPa rms pressure. Nevertheless, alternating voltage applied to the system is 1 volt for TVR while there is no such necessity for SL. Since the response of the transducer is linear under variable driving voltage, one can

obtain SL from TVR. TVR as well as SL can be expressed in terms of directivity index, efficiency and input electrical power, W_e [8]:

$$TVR = 10\log\left[\frac{W_e}{1watt}\right] + DI + 10\log(\eta_{ea}) + 170.8dB \tag{1.5}$$

where η_{ea} is the electroacoustic efficiency of the transducer and found simply by multiplication of electromechanical and mechanoacoustic efficiencies. For TVR, W_e must be calculated for a driving voltage of 1 volt. The SL could be easily calculated from TVR included the driving voltage of the transducer.

$$SL = TVR + 20\log\left(\frac{V_{drive}}{1volt}\right) \tag{1.6}$$

Bandwidth and beam width are the other important concepts for transducers which are used as design criteria according to the use of the transducer. Bandwidth is generally expressed as the absolute frequency difference of the points at which the SL or TVR value is 3 dB less than the peak value.

Beam width is a dB scale measurement of angular response of a transducer and it is directly related to the directionality of the transducer. Beam width can also be defined as the angle between directions where the response of the transducer is 3 dB less than the direction at which the maximum response occurs. This is generally the acoustic axis of the transducer.

Although beam width and directivity index of a transducer are both related with the directivity of a transducer, they are completely different terms. A transducer with high directivity index has narrow beam width; while a wide beam width means low directivity index.

1.5. General Information about Optimization

All engineering problems have many design variables which affect each other and even contradict with each other. To achieve a solution that satisfies the design requirements could be possible with the application of optimization algorithms. With the development of computer technology in recent years, use of optimization algorithms becomes widespread. Another reason for optimization algorithms becomes so popular is that algorithms could be applied in any field where there exists a minimization and maximization problem. A flowchart of optimization process is illustrated in Figure 4.

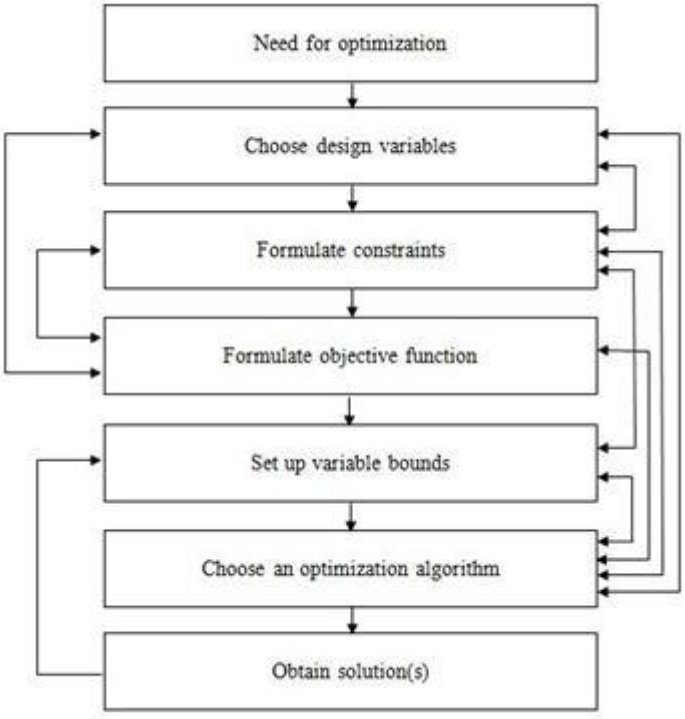

Figure 4: Flowchart Describing the Optimization Process

Optimization process begins with the formulation of the optimization problem. Since every engineering problem requires a different approach, it is almost impossible to apply a single procedure to all engineering problems [46]. However, an optimization algorithm accepts the problem in a specific format; so the problem should be formulated in that particular format.

As seen from Figure 4, the optimization process begins with the identification of the need for the optimization. Then, the design variables are required to be identified which are primarily varied during the optimization process. The efficiency and the speed of the solution largely depend on the number of design variables chosen [46].

After choosing design variables, the next step is to identify constraints associated with the optimization problem. The constraints represent some functional relationship among the design variables and other variables to satisfy certain physical and resource limitations. For instance, mechanical design problems have generally constraints to satisfy some stress or strain limitations.

There are two types of constraints: equality and inequality constraints. Generally, the constraints encountered during the optimization process are inequality type. Equality constraints state exactly that the functional relationship should be a resource value. Therefore, equality constraints are more difficult to handle and should be avoided. Instead, equality constraints should be tried to use in for the sake of reducing design variables.

One of the most important tasks for construction of optimization problem is to decide objection function. This is the function that should be minimized or maximized. The success of the optimization is directly related to the objective function specified.

Final step of formulation is to set the lower and upper limits of design variables to restrict the algorithm within these bounds. Not all problems require such limitations, since the constraints surround the feasible region.

Optimization algorithms can be classified into two main groups: traditional and nontraditional methods. Traditional methods can also divided into two according to their iteration methods. Direct methods do not employ any derivative of the objective function while gradient techniques are based on first and/or second derivative information. Traditional techniques are useful for problems with linear objection function. However, if the problem is multi-modal, discontinuous and nondifferentiable, they may give meaningless results [47]. For such complex engineering problems, nontraditional methods are more purposive. Genetic algorithm and simulated annealing are the most widely used nontraditional methods. In this study, the objective functions used for the optimization of the design parameters are complex and nondifferentiable functions; therefore a nontraditional algorithm, namely genetic algorithm is utilized throughout the study.

1.6. A Review on Genetic Algorithm

Genetic algorithms are computerized search and optimization methods based on natural genetics and selection. The method is first envisaged by Professor Holland in midsixties [46].

Genetic algorithms maintain and manipulate a family or population of solutions and implement a *survival of fittest* strategy in their search for better solution [47]. In general, the fittest individuals of any population tend to reproduce and survive to the next generation.

Genetic algorithms have six fundamental issues which are chromosome representation, selection function, genetic operators making up the reproduction function, the creation of the initial population, termination criteria and the evaluation function.

Chromosome representation is essential for describing each individual in the population of interest. The representation scheme determines how problem is structured in GA as well as the genetic operators used.

Another important role in genetic algorithms is to produce successive generations from selected individual. A probabilistic selection is performed based upon the individual's fitness such that better individuals have more chance to be selected. There are several selection processes: roulette wheel selection and its extensions, scaling techniques, tournament and elitist models and ranking methods [48].

CHAPTER 2

LITERATURE SURVEY

2.1. Studies about Transducer Design

Sonar transducers have been used since the first discovery of Langevin transducer in 1917. Beginning with those days designing sonar transducers has always been an issue since it is a complex procedure. Since the sonar transducers have both electrical and mechanical parts working together, design process is required to have a comprehensive knowledge about electrical design as well as the mechanical design processes.

For transducer design, there are several modeling techniques available in the literature. The simplest models are lumped parameter models. Since a lot of assumptions are made for modeling the transducer, the accuracy of lumped parameter models depends directly on the validity of these assumptions. However, they are still widely used since they provide a first insight about the design of transducers and their simplicity. In addition, lumped models may introduce applicable results for use in more advanced models [9]. The simplest lumped model of a transducer is the one degree of freedom spring-mass system [9]. Also, spring-mass systems with two degrees of freedom are available in the literature [4, 9]. Furthermore, lumped models could involve electrical components of a transducer as well as mechanical parts.

A design method called "*Electrical equivalent circuit*" is capable of modeling of mechanical and electrical parts in one circuit with the help of impedance and mobility analogies [10]. In literature, there are many studies regarding electrical

equivalent circuits. Mason introduced an electrical equivalent circuit model [16]. The model has then become a milestone and many other models are developed based on Mason's model. Krimholtz *et al.* [17], advanced Mason's model to obtain a more capable model. With this model, calculation of electrical input admittance for an arbitrary acoustic load becomes possible. In the study of Chubachi and Kamata [18], a new electrical equivalent circuit model, namely NKC equivalent circuit, originated from the equivalent transmission line model, is presented. This equivalent circuit model is also compared with Mason's equivalent circuit. Study by Tilman also describes an equivalent circuit model for electromechanical transducers [19]. In the study [20], equivalent circuit models for broadband transducers with two resonance frequencies are presented. Equivalent circuits of a molded free-flooded, radially polarized, piezoelectric shell, a Tonpilz wideband transducer and a piezocomposite transducer are modeled. Such equivalent circuits for different kinds of transducers are also available in literature [21]. In [21], Aoyagi *et al*. presented an equivalent circuit analysis of polyurea transducers. In addition, there exist some studies in literature which do not directly forms the electrical equivalent circuits of the whole transducer but only of the piezoceramics [22, 23].

Another analytical method for the transducer design is the matrix method where lumped model assumptions are not used. In other words, all components of transducers are modeled including the mass, stiffness and damping properties seperately. Therefore, matrix models are the most powerful analytical tools for the transducer design. Iula *et al.* [24] developed a matrix model for radial mode of thin piezoceramic rings. The model is capable of predicting the dynamic behavior of piezoeceramics when the two main surfaces are stress free. In study [26] a more comprehensive matrix method is introduced by the same authors. The developed 3-D model of cylindrical shaped piezoceramics is able to figure out both radial and thickness modes. Study [27] includes a 3-D matrix model of not only just piezoceramics, but also Langevin transducers. Mancic *et al.* [28] also proposed an approximated 3-D model of piezoceramics. However in the study, both radial and thickness modes of piezoceramics as well as coupling between them is modeled. To

achieve this, 5 port network representation (4 ports for mechanical and 1 port for electrical properties) is used for piezoceramics. An extended work involving a complete model of whole sandwich transducers is presented in [29]. In this model, 5 port network representation is used for piezoceramics and 4 port network representation is employed for mechanical parts.

The models for piezoceramic transducers are mostly dominated by the Finite Element Method (FEM), due to great match between theoretical model and experimental results. Vadde *et al.* [30], conducted a FEM-based performance analysis as well as characterization of a Tonpilz transducer. There are any other studies in the literature which exactly focus on FEM analysis of Tonpilz transducers [31, 32, 33, 34, 35, 36]. Commercial software such as ANSYS [31-34], COMSOL [30], ATILA [35], PZFlex [36], GENSAM [37] are shown to be exploited with great success. In order to design a broadband transducer which benefits from the flexural mode of head mass to obtain broadband response, FEM is used [32, 34] because other methods are incapable of modeling the coupling between the modes. In the study [30], the approaches for tuning of resonance frequency are examined. In [35, 36], transducers in air are analyzed as well as in water.

Beyond these models, there also exist other models available in the literature; such as Boundary Element Model (BEM) [38] and KLM circuits [53]. However, these models are barely used and just a few studies are reported.

In literature, there also exist some studies which deal with not just a transducer model, but in general the modeling process and comparison of the models. Smith [38], presents different modeling techniques: equivalent circuits and coupled finite element-boundary element methods. Also, advantages and drawbacks of these models are explained. Modeling techniques of finite element and transmission line matrix (TLM) method for axisymmetric acoustic transducer are discussed by Coates [39]. Problems encountered during design process and some possible solutions are described. Last, Teng *et al.* emphasized the difference between electrical equivalent circuit method and the finite element method [40].

2.2. Studies about Optimization of Sonar Transducers

Design of a Tonpilz transducer is a complex procedure including various design parameters. These parameters affect the design and characteristics of transducers in different ways. Even, parameters may contradict with each other [12, 13]. In addition, design process may possess other constraints other than contradiction of design parameters. For instance, a high source level is a desired property for most transducers. Lessening the mass of the head mass increases the source level, while the area of the active surface is kept constant. On the other hand, it results in a decrease in thickness which provokes flexural modes to occur. It is a situation that should be prevented in design because it means a null response. As a consequence, to obtain a design that satisfies the desired requirements is a challenging task. Therefore, optimization methods are used to achieve an optimal design.

Various approaches are developed to reach an optimum design. One method is to use topology optimization [41]. Silva *et al*. explains that achieving the required task in design procedure is related with resonance frequency, vibration modes and electromechanical coupling coefficient. All these parameters are associated with many factors, the most important of which are transducer shape, in other words topology, and material properties. The design problem is considered as an eigenvalue problem and topology of head mass is obtained by optimal distribution of solid and void. An optimal wideband solution could be reached by bending piezoelectric disk on the radiation surface of transducer according to Saijyou *et al.* [42]. In the study [43], structural parameters of transducers are optimized. The aim for optimization is to increase the radiated power and broaden the bandwidth. Reynolds et al. [44] use optimization techniques to transducers to maximize the acoustical output. Studies of Crombrugge et al. [45] and McCammon et al. [13] present nonlinear goal programming implemented in design process to broaden bandwidth. The aim of the study [12] is to obtain pareto-optimal solution sets for specified desired properties.

The goals for the use of optimization techniques in the transducer design process are to maximize the radiated acoustic power [13, 43, 44] and/or broaden the bandwidth [42, 43, 44]. Only studies [12, 41] describe a general technique for the desired optimum characteristics. Although topology optimization is used [41, 42], mathematical optimization algorithms such as genetic algorithm [12, 43] and nonlinear goal programming [13, 45] are preferred. Also, a study [44] uses different mathematical optimization techniques; namely multiobjective genetic algorithm, the elitist non-dominated sorting genetic algorithm and improved strength Pareto evolutionary algorithm and discusses advantages and disadvantages of them. To apply mathematical optimization, proper models should be constructed. Electrical equivalent circuits are preferred generally [13, 43, 45]. There is only one study which uses FEM method for optimization [44]. Also, only one other study develops a matrix model depending on the rod theory.

Among all the studies expressed above, the optimized parameters are dimensions of head mass [12, 13, 41, 42, 43, 44], piezoceramic stack [12, 43, 44] and tail mass [12, 13, 43, 44]. In addition material properties are used for design variables [12, 45].

CHAPTER 3

TRANSDUCER MODELS

3.1. Lumped Parameter Model

Simplest models in existing literature about transducer design are the lumped parameter models. In lumped model approach, head and tail masses are assumed to be ideal rigid masses and undergo no bending or compression while the piezoceramic stack is analogous to ideal massless spring [4, 8, 9]. In addition, dimensions of the physical elements are assumed to be less than one quarter of the corresponding wavelength essentially. Other transducer parts such as stud, glue and insulators are simply ignored. Although not being very accurate, lumped parameter models are still powerful tools as starters of transducer design process.

In this section, a simple mechanical lumped model is introduced. The aim of this model is to obtain the main transducer dimensions with respect to the desired resonance frequency and bandwidth. After obtaining the rough dimensions, fine tuning of the dimensions of the transducer can be achieved by utilizing the more detailed and accurate models.

Figure 5 shows a sketch of a two-degree of freedom spring-mass-damper system. This system basically represents a Tonpilz type transducer with M_h as head mass, M_t as tail mass. Also, K_e is analogous to the stiffness of the ceramic stack where R_h is analogous to radiation resistance. Force is applied onto both head and tail mass from piezoceramic section.

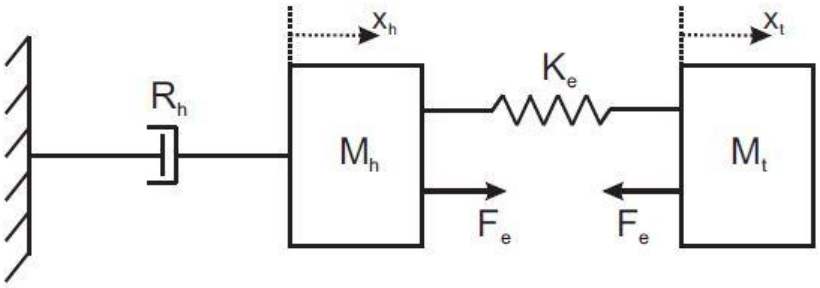

Figure 5: Sketch of a Two-degree of Freedom Spring-Mass-Damper System [9]

The corresponding equations of motion for this two-degree of freedom spring-mass-damper system are obtained as [14]:

$$M_h \frac{d^2 x_h}{dt^2} = F_e + (x_t - x_h)K_e - R_h \frac{dx_h}{dt} \tag{3.1}$$

$$M_t \frac{d^2 x_t}{dt^2} = -F_e - (x_t - x_h)K_e \tag{3.2}$$

With the approximation of $R_h << \omega(M_h + M_t)$, the system can be reduced to a single degree of freedom system for ease of analysis:

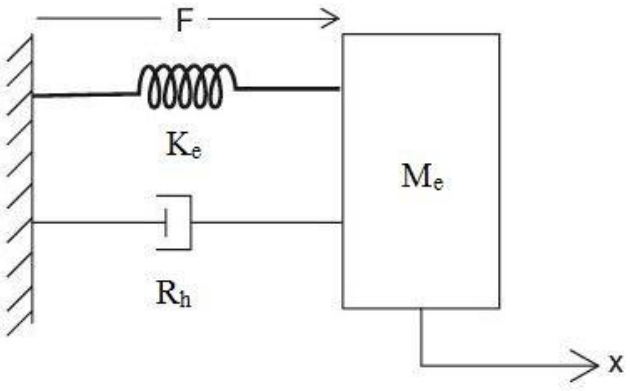

Figure 6: Sketch of a Single Degree of Freedom Spring-Mass-Damper System [4]

Equations of motion for the system shown in Figure 6 are expressed as follows:

$$M_e \frac{d^2x}{dt^2} + R_e \frac{dx}{dt} + K_e x = F_e \tag{3.3}$$

$$M_e \frac{du}{dt} + R_e u + K_e \int u dt = F_e \tag{3.4}$$

where $u = dx/dt$. In these equations, K_e represents the stiffness of the piezoceramic stack, M_e is the effective mass and R_e is the effective damper. The corresponding equations for M_e and R_e are as follows

$$M_e = \frac{M_h M_t}{M_h + M_t} \tag{3.5}$$

$$R_e \approx \frac{R_h}{(1 + M_h / M_t)^2} \tag{3.6}$$

Circular undamped natural frequency and natural frequency can be obtained for this system as:

$$\omega_n = \sqrt{\frac{K_e}{M_e}} \tag{3.7}$$

$$f_n = \frac{1}{2\pi} \sqrt{\frac{K_e}{M_e}} \tag{3.8}$$

Resonance frequency can be taken as the undamped natural frequency for light damping. The mechanical quality factor, Q_m, of the reduced system is defined as follows:

$$Q_m = \frac{\omega_n M_e}{R_e} \tag{3.9}$$

The mechanical quality factor, Q_m, is also defined as the ratio of resonance frequency to the bandwidth.

$$Q_m = \frac{f_n}{\Delta f} = \frac{f_n}{f_1 - f_2} \tag{3.10}$$

where f_1 and f_2 are the half power frequencies at which the responses are half of the resonance frequency; therefore, Δf is bandwidth.

Combining Equations 3.5, 3.6, 3.7 and 3.9, the mechanical quality factor and the circular resonance frequency could be found as follows:

$$Q_m = \frac{\sqrt{K_e M_h}}{R_h}\left(1 + \frac{M_h}{M_t}\right)^{1.5} \tag{3.11}$$

$$\omega_n = \sqrt{K_e\left(\frac{M_h + M_t}{M_h + M_t}\right)} \tag{3.12}$$

One can obtain rough dimensions of the transducer from Equations 3.11 and 3.12 with the help of some extra concepts, such as tail-to-head mass ratio, κ_{th}:

$$\kappa_{th} = M_t / M_h \tag{3.13}$$

Although the designer decides the tail-to-head mass ratio; in literature reasonable tail-to-head ratio is recommended as between 1 and 10 while the typical values range between 2 and 4 [9]. The ratio is simply indicator of the ratio of the vibration velocities of the tail mass to the head mass. Larger the ratio results higher the vibration velocity of the head mass as well as radiated acoustic power. Therefore,

higher tail-to-head mass ratio is preferable. On the other hand, it causes heavier transducer which is generally undesirable.

The unknowns K_e, M_h and M_t could be found by means of Equations 3.11-3.13. However, first of all the radiation resistance, R_h, has to be decided. Radiation resistance depends on shape and dimensions of the active surface. The shape of the active surface can be decided according to application of the transducer. Circular shape is usually preferred since it is more advantageous in concern with flexural resonance. Nevertheless, square and hexagonal shaped transducers are favored in array applications, because they can provide fully-covered array surfaces.

Radiation resistance is equivalent to the radiated acoustic power into the acoustic medium. During design process, radiated acoustic power; in other words, radiation resistance, is aimed to be maximized. As a result, to fix the radiation resistance, an ideal case for acoustic applications, namely, radiation impedance for a circular piston in a rigid baffle should be considered. Further information about radiation resistance could be found in Appendix A.

Avoiding the flexural resonance since it causes null response is another requirement of the design process. To check the flexural resonance, one should find the thickness of the head mass. Thickness could be found from:

$$t_h = \frac{M_h}{A_h \rho_h} \tag{3.14}$$

where A_h is the area of the active surface, ρ_h is the density of the head mass. Area of the active surface is found from the radiation resistance. To find the density, the material of the head mass should be decided first. Head mass is desired to be lightweight compared to the tail mass due to high acoustic power requirements. In addition, acoustic impedance of the head mass needs to be between the acoustic impedances of water and piezoceramics. Consequently, low density materials such as aluminum, beryllium alloys, magnesium can be chosen [4].

After the thickness of the head mass is determined, flexural resonance should be checked. The corresponding equation for flexural resonance frequency is given by:

$$f_{flex} = \frac{1.65ct_h}{4a^2\sqrt{(1-\nu^2)}} \tag{3.15}$$

The flexural resonance frequency should be much higher than the central frequency. Practically, it should be at least twice of the resonance frequency [9]. If the frequency is lower than 2 times of the resonance frequency, the procedure is required to be repeated until the targeted value is achieved.

Subsequently, dimensions of tail mass and ceramic stack need to be acquired. From previously determined tail-to-head mass ratio, the mass of the tail mass could be found easily. The material of the tail mass has to be decided first to obtain the dimensions of the tail mass. The tail mass is required to be higher than the head mass. In order to volume not to be an issue, materials with high density, such as steel and tungsten, are preferred to be chosen as tail mass material. The simplest element of the transducer is the tail mass, since its only duty is to provide the required mass and undergoes no other constraint as in the case of head mass. The only constraint for the tail mass is that any dimension has to be shorter than quarter of the wavelength. After defining the radius of the tail mass, r_t, the last dimension of the tail mass, i.e. its length could be found from:

$$l_t = \frac{M_t}{\rho_t \pi . r_t^2} \tag{3.16}$$

For ceramic stack dimensions, first the ceramic material has to be selected. Afterwards, knowing the value of K_e, which is the stiffness of the ceramic stack, the area-to-length ratio of the piezoceramic stack could be easily found by means of the formula below:

$$K_e = \frac{E_{pzt} A_{pzt}}{l_{pzt}} \qquad \frac{K_e}{E_{pzt}} = \frac{A_{pzt}}{l_{pzt}} \tag{3.17}$$

To decide area and length of the piezoceramic stack, one can utilize a practical concept of ratio of the area of the ceramic stack to the area of the head mass. From literature, this ratio could be decided as [4]:

$$A_h / A_{pzt} = 5 \tag{3.18}$$

Equation 3.18 helps to settle the area of the piezoceramic stack. Then, the length of the stack could be easily found from Equation 3.17. The only unknown physical dimensions of the ceramic stack are inner and outer diameters of the ceramics. To determine the diameters, Equations 3.19 and 3.20 could be used.

$$r_{pzt\_mean} = \sqrt{\frac{A_{pzt}}{\pi}} \tag{3.19}$$

$$A_{pzt} = \pi(r_{mean\_pzt} + \Delta r_{pzt})^2 - \pi(r_{mean\_pzt} - \Delta r_{pzt})^2 \tag{3.20}$$

3.2. Electrical Equivalent Circuit Model

Electrical equivalent circuit models have a widespread use in transducer design because not only the mechanical parts, but also the electrical parts can be modeled with equivalent circuit models. Underwater transducers are electromechanical devices that electrical and mechanical parts work together and may affect performances of each other's; one circuit can be used to represent the whole transducer for convenience. Another advantage of this modeling technique is that the designer has some freedom in detailing the model. For instance, the designer could involve additional parts such as stud, glue excluded from lumped mechanical model. Because of such benefits, electrical equivalent circuit models have been widely used in studies.

Mechanical parts of the transducer could be implemented into the electrical circuit with the help of impedance analogy. Mechanical terms with their electrical equivalents according to impedance analogy are tabulated in Table 1, below:

Table 1: Mechanical Terms with their Electrical Equivalents

Mechanical Terms	Electrical Equivalents
Force	Voltage
Velocity	Current
Mass	Inductance
Damper	Resistance
Compliance (1/Stiffness)	Capacitance

In this section, an electrical equivalent circuit explained in [4] is used. This model is also based on lumped parameter representation. However, some additional components as well as electrical parts can be included in the model. Therefore, the model is more accurate compared to the lumped parameter mechanical model. Figure 7 shows a basic lumped transducer model.

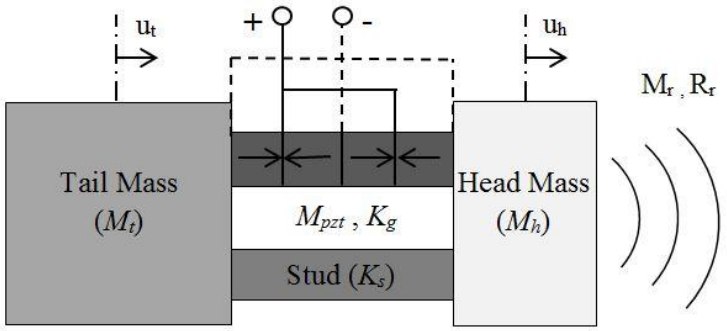

Figure 7: Basic Lumped Transducer Model

The corresponding electrical equivalent circuit of the basic lumped parameter transducer presented above, is displayed in Figure 8.

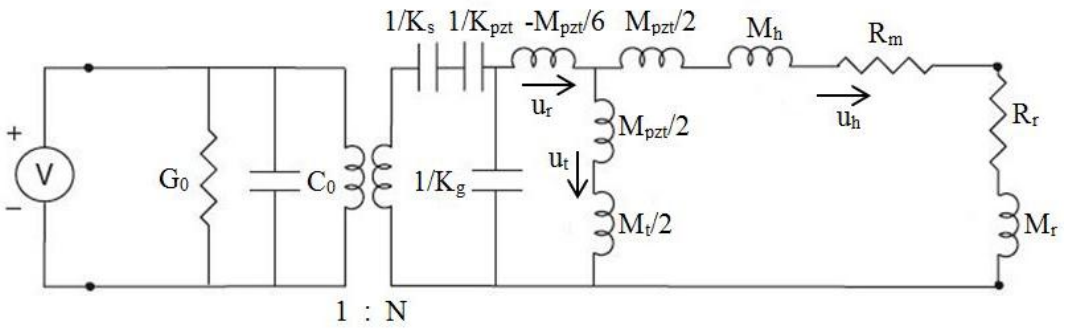

Figure 8: Electrical Equivalent Circuit of the Basic Lumped Transducer Model

The term *N* is called the transformation/transformer ratio or transduction coefficient [4, 8, 9]. It is the indicator of the relationship between the applied voltage and the obtained force. It can be defined as $N = F/V$ basically. However, for electrical equivalent circuit calculation, another definition which depends on properties of the piezoceramic material is essential. Such a definition which can be found in literature [9] is given by:

$$N = \frac{d_{33} A_{pzt}}{s_{33}^{E} t_{pzt}} \tag{3.21}$$

where A_{pzt} is the cross-sectional area of the ceramic stack, t_{pzt} is the thickness of one(?) ceramic. D_{33} and s_{33}^{E} are constants describing piezoceramic material properties. The subscript *"33"* means that the applied voltage and the motion occur in the same direction.

M_h, M_t and M_{pzt} are masses of the head mass, tail mass and the piezoceramic stack, respectively. Since piezoceramics are very dense materials, the mass of the ceramic stack can affect the transducer behavior. The mass of the ceramic stack is divided into two and added both to the head mass and the tail mass. The out-of-phase motion of the head mass and the tail mass can also be understood from the equivalent circuit. The vibration velocities of the head mass and the tail mass, u_h and u_t respectively, are opposite in direction. In addition, the parallel arrangement of the head and the tail masses implies that the same magnitudes of forces are applied onto the head and the tail masses.

K_{pzt} and K_s are the stiffness terms belonging to the piezoceramic stack (when applied electric field is 0) and the stud, respectively. Besides, K_g is stiffness regarding to the glue which is used to unify the ceramics behaving like a cement joint. Therefore, its stiffness is added to the system. K_s and K_{pzt} are connected in series in the circuit. The forces applied to get spring deformations are proportional with the magnitude of their stiffnesses, obviously. Therefore, the stiffer the stud, the more force required for its displacement would be. As a result, the stiffness of the stud better to be as low as possible in order not to affect the transducer response. The ratio of K_{pzt}/K_s ranges between 5 and 15 [8].

In the circuit, R_r and M_r are radiation resistance and radiation reactance, in other words; real and complex parts of the radiation impedance, respectively. Radiation impedance depends both on wavelength and geometrical shape of the transducer. For this level of modeling an analytical approach which assumes the velocity of the head mass as uniform can be used. The detailed explanation of analytical approach is given in Appendix A.

The radiation impedance terms, R_r and M_r are connected in series to the head mass term since the radiation impedance is obtained due to displacement of the head mass. Inherently, vibration velocities are the same.

The term C_0 is defined as the *clamped capacitance*. For the *clamped* condition, the strain in the direction of the applied electric field is kept zero. In other words, the motion in direction of the applied electric field is not allowed. With the same approach, the *free capacitance* is basically capacitance in the condition when the stress in the direction of applied electric field is zero. Free condition means that the piezoceramics is not restricted when the electric field is applied. The relationship between the C_0 and C_f can be seen below:

$$\frac{C_0}{C_f} = 1 - k_{33}^{\ 2} \tag{3.22}$$

where k is called the *electromechanical coupling coefficient*. It is the ratio of the transduced mechanical energy to the input electrical energy. Materials with high k are preferable, because they show better piezoelectric properties. The subscript of the coefficient implies the direction of the applied electric field and direction of the strain in the material. For 1-D case, the definitions of C_f and k_{33} can be expressed as follows:

$$C_f = \frac{n\varepsilon_{33}^{\ T} A_c}{t_c} \tag{3.23}$$

$$k_{33} = \frac{d_{33}}{\sqrt{s_{33}^{\ T}\varepsilon_{33}^{\ T}}} \tag{3.24}$$

The term R_0 represents the electrical resistance of the transducer due to piezoceramic rings. Piezoceramics can be considered as capacitors electrically. Parallel connection of piezoceramics causes resistance which is responsible for the electrical leakage. If other resistances due to electrical connections, cables, etc. are ignored; the only resistance is R_0 which will also be equal to the electromechanical efficiency, η_{em}, of the transducer. The mathematical representation of this term is given below:

$$R_0 = \left(\omega C_f \tan\delta\right)^{-1} \tag{3.25}$$

Last, the term R_m is defined as the internal mechanical resistance of the transducer. The mechanical resistance depends on assembly details and increases with the frequency [9]. For better acoustical performance, it should be kept as low as possible compared to the radiation resistance. Their relationship determines the mechanoacoustical efficiency:

$$\eta_{ma} = \frac{R_r}{R_r + R_m} \tag{3.26}$$

Electromechanical and mechanoacoustical efficiencies together set down the overall efficiency of the transducers.

3.3. Finite Element Model

Finite element models are the most accurate and therefore, the most reliable modeling technique for transducer design as well as other mechanical design processes. Analytical methods can offer solutions with simplified problems and simple geometrical properties. Even a small amount of complexity in the problem causes difficulty in solution of the problem [9]. FE methods overcome these types of problems with division of problem domain into small elements to which obtaining analytical solutions is not problematic. On the other hand, FE methods present only approximate solutions. Accuracy of the solution is based on the element size of the model. Larger element numbers lead to smaller elements and a better continuity. As a result, the solution becomes more accurate. However, beyond a limit, increasing element numbers would not affect the solution, but cause large errors due to error accumulation for each element.

In addition, correct definition of material properties has a crucial importance on the accuracy of the FEM solution. The required material constants change according to the analysis type. For harmonic analysis of piezoacoustic transducers conducted in this study, it is required to define isotropic materials, piezoceramics and acoustic medium [9]. For isotropic materials, three material properties, namely, modulus of elasticity, Poisson's ratio and density are sufficient. On the other hand, stiffness matrix, piezoelectric matrix and dielectric matrix, all defined according to polarization direction and density, are required for piezoceramics. Definition of acoustic medium is limited to definition of sonic speed and density.

ANSYS can be applied to carry out the acoustic analysis, which includes the generation, propagation, scattering, diffraction, transmission, radiation, attenuation, and dispersion of sound pressure waves in a fluid medium. In addition, ANSYS supports harmonic response analysis due to harmonic excitation [49]. In such an analysis, the steady-state response of the transducer subjected to an alternating voltage is computed in a definite frequency range. The procedure for harmonic response analysis involves four major steps.

The first step is building model. This step includes constructing the geometry of the model; assign materials to parts of the transducer and dividing transducer parts into finite elements. Also, defining the element type for these materials is very crucial considering the accuracy of the solution.

Second, boundary conditions which are all forces, connections and boundary conditions have to be applied to the model at this stage. Since both forces and connections have a great impact on solution, for an acceptable solution, boundary conditions of the systems should be carefully analyzed and implemented to the simulation.

The third step is obtaining the solution. At this stage, all governing algebraic equations in matrix form are solved for elements in the model simultaneously. The

unknowns, degrees-of-freedom elements such as displacement, pressure and voltage are obtained.

Last, the results are checked. For this stage, different results could be obtained by solving the necessary set of equations.

As discussed above, the definition of element types affects the correctness of the FEM solution directly. ANSYS has many element types for different kind of materials and analyses. Element type of FLUID29 is used for acoustic medium since it includes pressure and displacement DOF's. However, the displacement DOF's are available only for the nodes at the fluid structure interface. For isotropic materials except head mass, such as tail mass, stud and nut material, PLANE82 elements reveal correct results. PLANE82 elements supply 8 nodes in an element including midnodes. Although material of the head mass is also isotropic, for head mass PLANE42 elements with four nodes are used to avoid errors due to fluid structure interface. Since piezoceramics also require an additional DOF for voltage, PLANE223 elements are used.

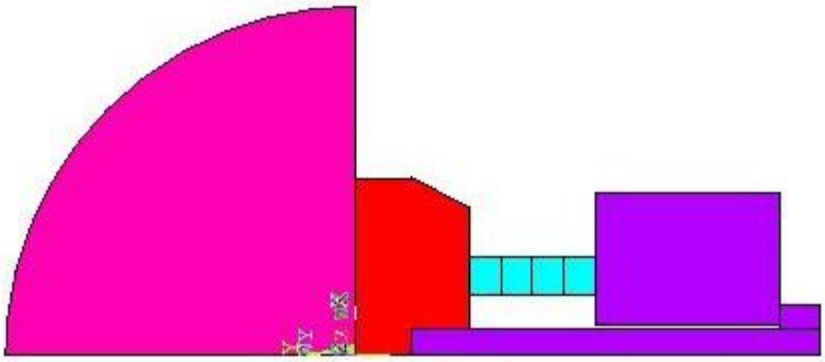

Figure 9: FEM of Tonpilz-type Transducers with Water Loading

While analyzing of the piezoelectric underwater transducers, not only coupled behavior of the piezoceramics, but also the interaction of unbounded media as well as material damping of the transducers should be taken into account. For simulation, the unbounded media has to be truncated into a finite region near transducer. However, at the truncated boundary, an artificial reflection could occur which affects the solution [50]. Therefore, it is essential to accomplish a transparent boundary to avoid artificial reflection. ANSYS supplies FLUID129 elements which can absorb outgoing pressure waves reaching the boundary of the model and prevents artificial reflection at the acoustic boundary. The placement of absorbing boundary at a distance of 0.2λ beyond the region can produce accurate solution [49]. Another important case is the boundary between the active surface and the acoustic medium. Fluid structure interface is where the displacement DOF of the active surface elements.

CHAPTER 4

VALIDATION AND COMPARISON OF MODELING TECHNIQUES

The models described in Chapter 3 were validated by means of the in-water measurements of a 50 kHz Tonpilz transducer by Bayliss [51]. As discussed in the thesis, the transducer is designed by J. R. Dunn [52]. These results belonging to Tonpilz transducer with resonance frequency of 50 kHz are also used in MS thesis by Çepni [9]. In Figure 10 the Tonpilz transducer from Bayliss' study and its 3-D model taken from Çepni's study are illustrated.

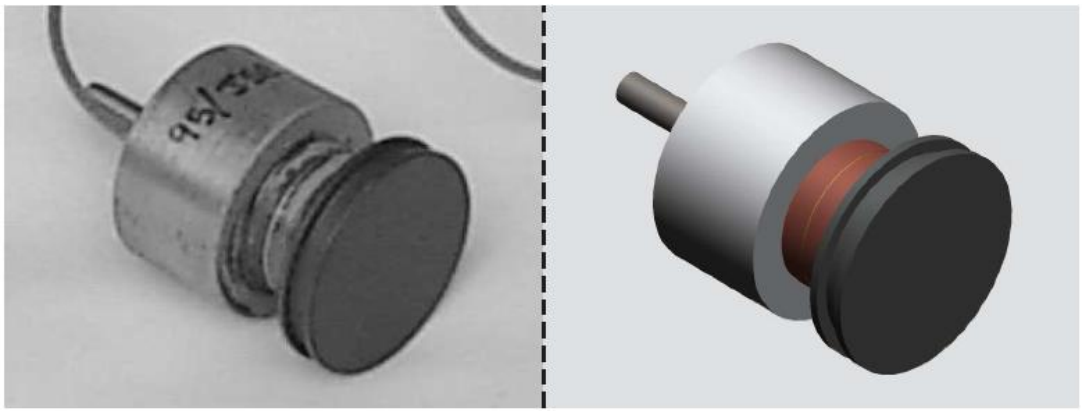

Figure 10: 50 kHz Tonpilz Transducer from Bayliss Study: (a) Real [51] and (b) Model [9]

The detailed geometrical and material properties of the 50-kHz Tonpilz transducer can be investigated from Çepni's study [9]. The head mass is made from hard anodized aluminum. The tail mass is from mild steel while stainless steel is used for the stud and nut. Last, the transducer is driven via PZT-4 ceramics.

To validate the models, the conductance and TVR results of the 50-kHz Tonpilz transducer are used. Conductance, *G*, being an electrical term is an appreciated indicator of the resonance frequency. The resonance frequency of a transducer is simply the frequency at where the conductance response gets its maximum value. TVR is also taken into consideration during the benchmarking procedure because it demonstrates the performance of a transducer.

To compare the results obtained via models in Chapter 3 and the measurements conducted in Bayliss' dissertation, the conductance and TVR graphics should be digitized. The digitization procedure is conducted with the software Engauge Digitizer. Below, converted graphics of conductance response (Figure 11) and TVR are presented (Figure 12).

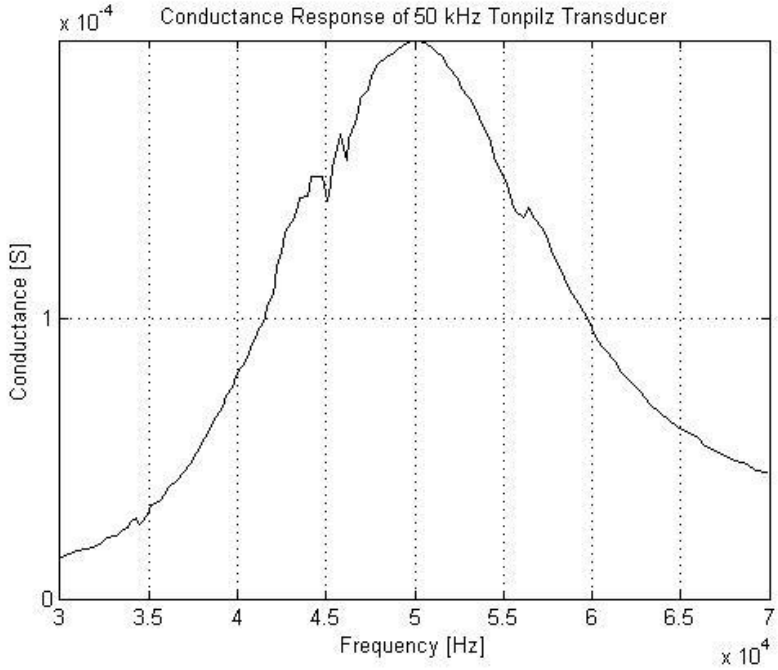

Figure 11: Conductance Response of 50-kHz Tonpilz transducer

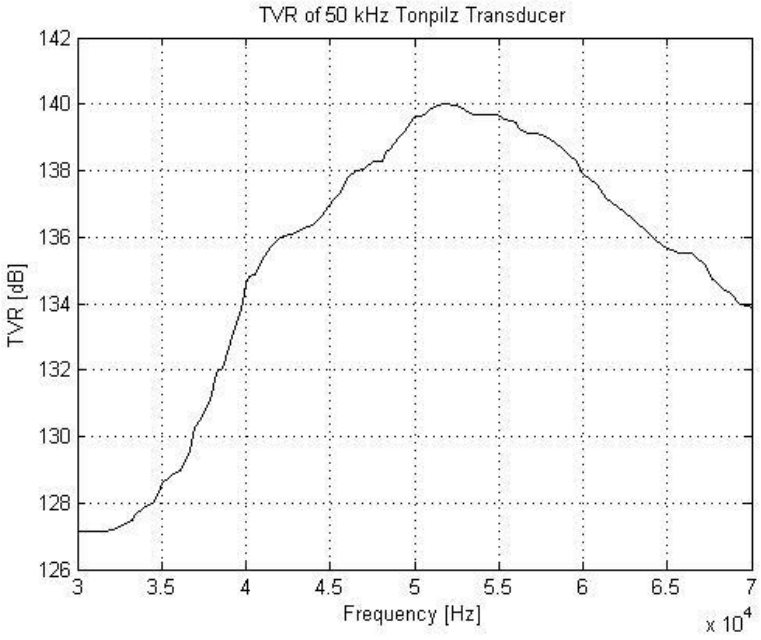

Figure 12: TVR of 50-kHz Tonpilz Transducer

4.1. Validation of Lumped Parameter Model

As mentioned in Chapter 2.1, simple lumped parameter model is specifically constructed for the goal of obtaining an initial approximation of design parameters. Being different from other models, the outputs of this simple lumped parameter model are design parameters, not TVR and conductance response. Therefore, the validation through TVR is not applicable for this model. However, the resonance frequency obtained via simple lumped parameter model can be compared with the resonance frequency attained with the conductance response.

Exact dimensions of reference 50-kHz Tonpilz are available in Bayliss' dissertation. First, these dimensions are used to obtain rough dimensions of transducer. Then, natural frequency of the reference transducer is found via Simple Lumped Parameter Model and the results are compared to find the accuracy of the model. The required properties are M_h, M_t and K_{pzt}. In order to find these properties, 3D CAD models of tail and head masses are prepared according to dimensions

presented in Bayliss' PhD thesis. The volumes and masses of head and tail masses are presented in Table 2:

Table 2: Rough Dimensions of Head and Tail Masses of Reference 50-kHz Tonpilz Transducer

	Volume [m^3]	Mass [kg]
Head Mass	2.826E-6	7.66E-3
Tail Mass	6.567E-6	50.57E-3

Hence the effective mass of the reference transducer could be found from Equation 3.5:

$$M_e = \frac{M_h M_t}{M_h + M_t} = 6.65 \times 10^{-3} kg$$

The effective stiffness, K_e, is the stiffness of the piezoceramic stack. Considering the material properties of piezoceramics and the geometrical properties of the stack, stiffness could be acquired as below:

$$K_e = \frac{A_{pzt}}{t_{pzt} n_{pzt} s_{33}^E} = 1.083 \times 10^9 N/m$$

The resonance frequency of the transducer is calculated simply as:

$$f_n = \frac{\omega_n}{2\pi} = \frac{1}{2\pi}\sqrt{\frac{K_e}{M_e}} = 64.2 kHz$$

The measurement and the Lumped Parameter Model results regarding the resonance frequency of reference 50-kHz Tonpilz transducer and the relative percentage error are represented in Table 3:

Table 3: Measurement and Simulation Results of Simple Lumped Parameter Model

	Measurement	Simulation	Relative Error [%]
Resonance Frequency (f_n)	50 kHz	64.2 kHz	28.4

Since the Lumped Parameter Model includes a significant number of assumptions, the error regarding to measurement and simulation results is as high as 28.4%. Although the error is high, the model is still reasonable because the aim of the model is to give an initial guess on dimensions of transducer.

4.2. Validation of Electrical Equivalent Circuit Model

For benchmarking of the Electrical Equivalent Circuit Model, both TVR and conductance response is applicable for the interested frequency band. Application of this model contains representation of transducer as an electrical circuit. Therefore, conductance response is achieved easily. On the other hand, certain assumptions should be made to acquire TVR of the model. The first assumption is that the head mass of the transducer vibrates with a uniform velocity like a piston. Any flexural motion is neglected. Second assumption is that the plane wave acoustic intensity is available at 1 m away from the transducer which is very reasonable for 50 kHz transducer. The TVR can also be obtained from the model with the help of the following formulation:

$$TVR = 10\log(W_a) + DI + 170.8dB \tag{4.1}$$

where W_a is radiated acoustic power in watts and *DI* is the directivity index. The formulation of *DI* introduced with Equation 1.4 for the case of a circular piston in a rigid baffle can be used in Equation 4.1, as the head mass of the reference transducer is assumed to vibrate with a uniform velocity. The radiated acoustic power, W_a, can be calculated from Equation 4.2.

$$W_a = |u_{rms}|^2 R_r \tag{4.2}$$

where u_{rms} is the root mean square vibration velocity of the active surface and R_r is the radiation resistance of the regarding surface. Radiation resistance term of the circuit presented in Figure 8 can be calculated from equations of radiation impedance of circular piston in a rigid baffle. The current on the branch of radiation resistance can be treated as the root mean square vibration velocity since velocity is equivalent to current according to impedance analogy.

The existing parameters of the electrical circuit represented in Figure 8, have to be calculated first to run the model. Electromechanical and mechanoacoustical efficiencies of transducer are difficult to determine accurately since they are identified according to the assembly of the transducer. Therefore, , the model is assumed to be ideal without any losses, that is, with all efficiency terms taken as 1 in this simulation. The R_0 and R_m of the circuit are taken as zero. For the values regarding to the mass of head and tail masses, M_h and M_t, in Figure 8, the mass terms calculated in Chapter 4.1 can be used. Likewise, for the stiffness of the ceramic stack, K_{pzt}, 1.083×10^9 *N/m* is used as found in Chapter 4.1., since they are identical. In addition to these, the mass of the ceramic stack has to be calculated. From the dimensions of the ceramic stack and the material properties, the mass of the ceramic stack is determined as $M_{pzt} = 4.53 \times 10^{-3}$ *kg*. The stiffnesses of glue between ceramics and stud, K_g and K_s are estimated as 5.456×10^9 N/m and 6.919×10^7 N/m, respectively. The transduction coefficient can also be found with the help of Equation 3.21:

$$N = \frac{d_{33} A_c}{s_{33}^E t_c} = 0.626 \ \ N/V$$

The last term of the circuit shown in Figure 8 is the clamped capacitance of the piezoceramic stack, C_0, which can be calculated from combining Equations 3.22, 3.23 and 3.24:

$$C_0 = \frac{n \varepsilon_{33}^T A_c}{t_c} (1 - k_{33}^2) = 3.942 \times 10^{-10} \ F$$

As the results of reference 50-kHz transducer are available in the frequency range of [30, 70] kHz, the model is run for this frequency range. The in-water conductance and transmitting voltage responses of the Electrical Equivalent Circuit Model and the reference transducer are presented in Figure 13 and Figure 14. Also the results and the relative percentage error regarding to the results are tabulated as observed from Table 4.

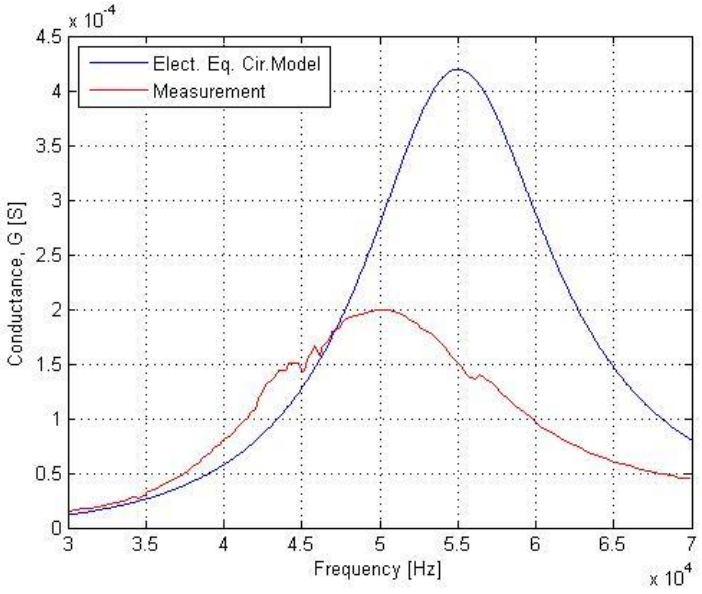

Figure 13: In-water Conductance Responses of Electrical Equivalent Circuit Model and Reference 50-kHz Tonpilz Transducer

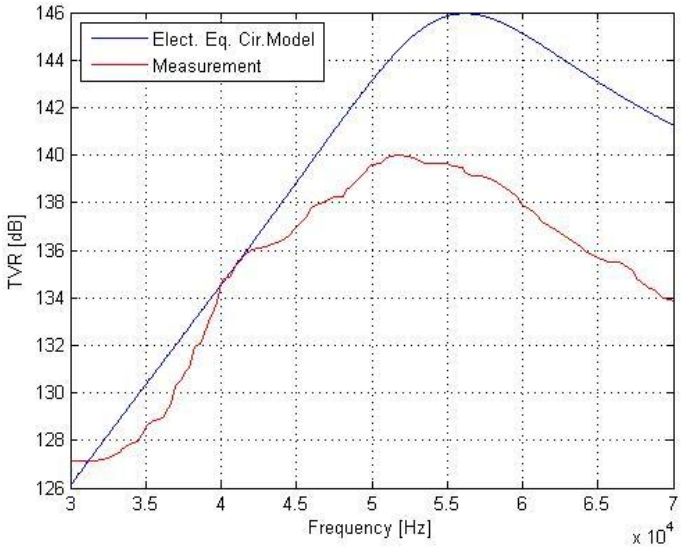

Figure 14: TVR of Electrical Equivalent Circuit Model and Reference 50-kHz Tonpilz Transducer

Table 4: Comparison of the Measurement and Electrical Equivalent Circuit Model Results

	Measurement	Simulation	Relative Error [%]
Resonance Frequency (f_n)	50 kHz	55 kHz	10
TVR	140.06 dB	145.95 dB	4.2

The error regarding to Electrical Equivalent Circuit Method is 10% on the basis of the conductance response. This result is expected since model is constructed from lumped parameters. Consequently, one can say the model eases calculations; although employment of lumped parameters causes high degrees of error.

4.3. Validation of Finite Element Model

Finite Element Model is the most comprehensive among all the models introduced in Chapter 3 since no major geometrical assumptions have to be made. Modeling of the reference 50-kHz transducer with finite element model does not involve any major simplification of geometry. An axisymmetric model is beneficial. The nut is modeled as a hollow cylinder instead of a hexagon nut and the holes in the tail mass for the cables are ignored. In addition, very thin elements such as electrodes and insulators between piezoceramic stack and head and tail masses are neglected since these elements may cause errors and difficulty in meshing process. Figure 15 shows the finite element geometry of the reference transducer.

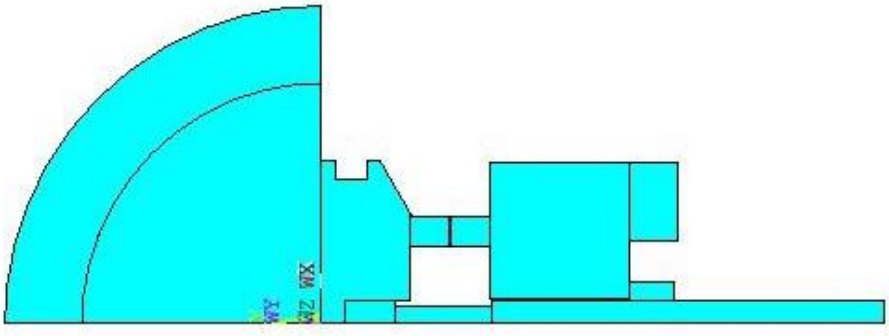

Figure 15: Finite Element Model of Reference 50-kHz Transducer

One of the most important steps in finite element modeling is to decide the element size. It is expected that smaller element size produces more accurate solutions. However, it also causes high round-up errors and therefore imprecise solutions. A convection study is conducted to define the correct element size. The FE model is meshed with different element sizes. The resonance frequency results and the error regarding the resonance frequency results of FEM with respect to element size are presented below (Figure 16 and Figure 17):

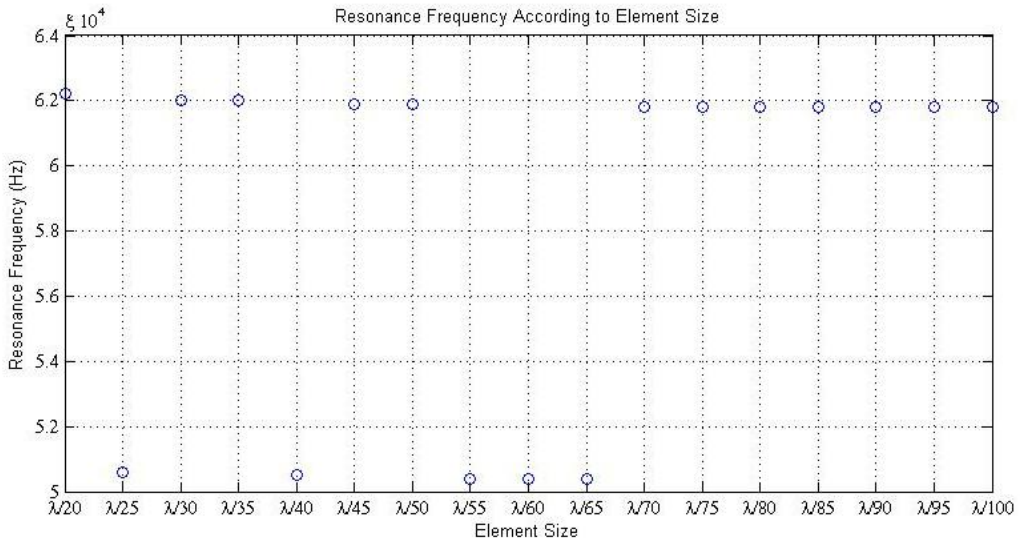

Figure 16: The Resonance Frequency Response of FEM of the Reference Transducer with respect to Element Size

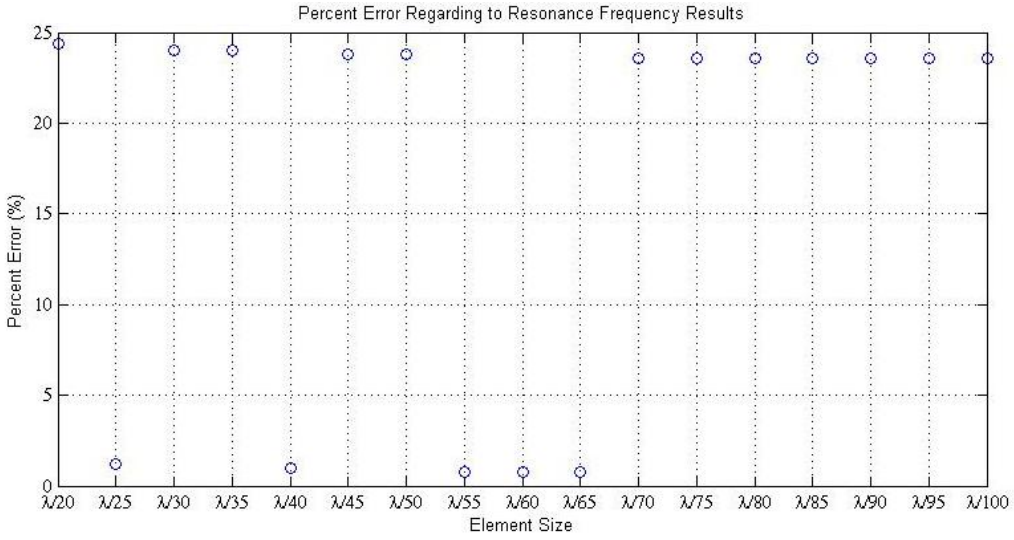

Figure 17: The Error Regarding to Resonance Frequency Response of FEM of the Reference Transducer with respect to Element Size

Also, transmitting voltage responses of simulation and measurement are compared. Figures 18 1nd 19 show the TVR according to the element size of the FE model and the regarding error:

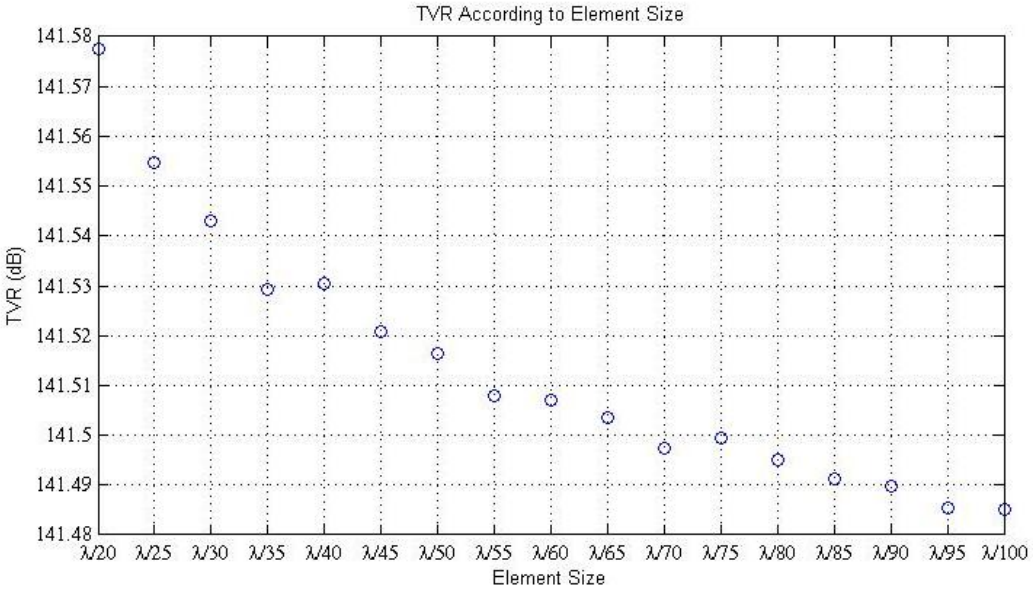

Figure 18: TVR of FEM of the Reference Transducer with respect to Element Size

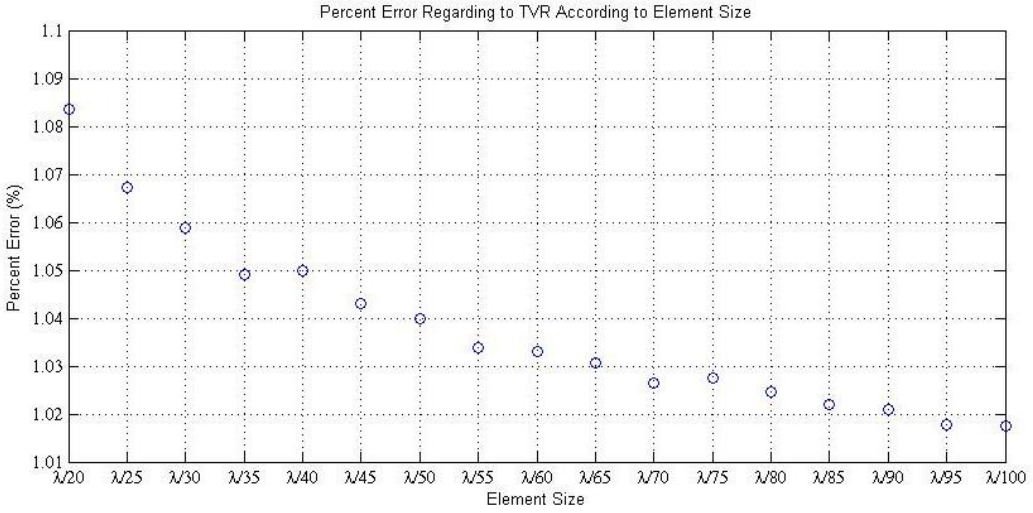

Figure 19: Error Regarding to the TVR of FEM of the Reference Transducer with respect to Element Size

From Figure 16 and Figure 17, it is deduced that range of element size λ/55 – λ/65 yields the closest resonance frequency response result to the measurement among the range of λ/20 – λ/100. In addition, when the TVR results are inspected, it is

concluded that TVR does not change considerably. As seen from Figure 19, the percent error differs between 1.0185-1.0835 %. Therefore, an element size of λ/60 is decided for FE model. The meshed FE model of the reference 50-kHz transducer is represented in Figure 20:

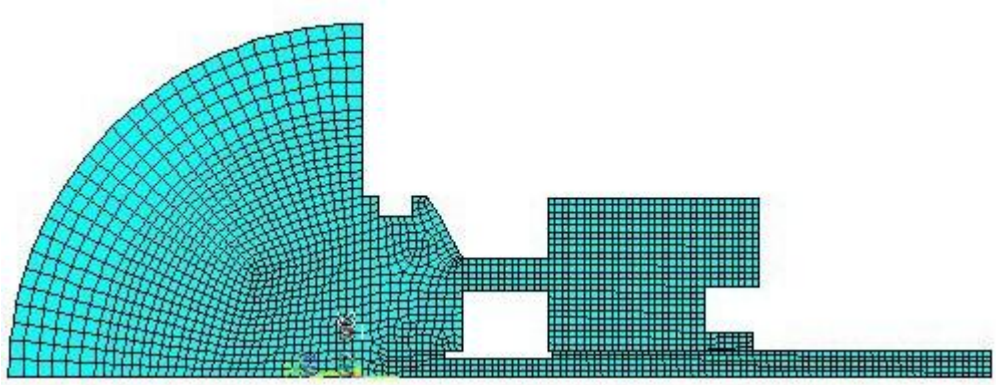

Figure 20: Meshed FE Model of the Reference 50 kHz Transducer

The resonance frequencies and TVRs of measurement and simulation are compared in Table 5. Also, Figure 21 and Figure 22 show conductance response and TVR results of the simulation executed with the help of FEM.

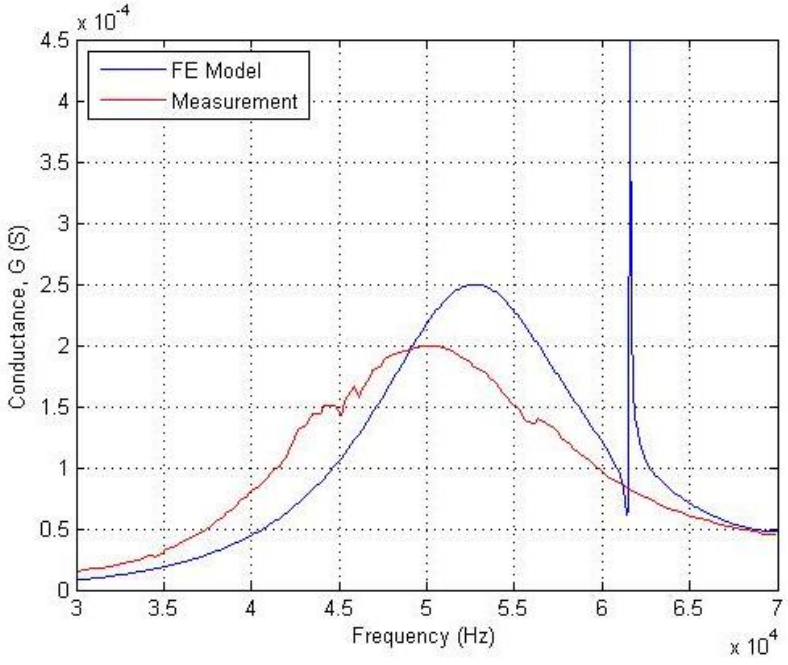

Figure 21: Conductance Responses of FE Model of the Reference Transducer and the Measurement

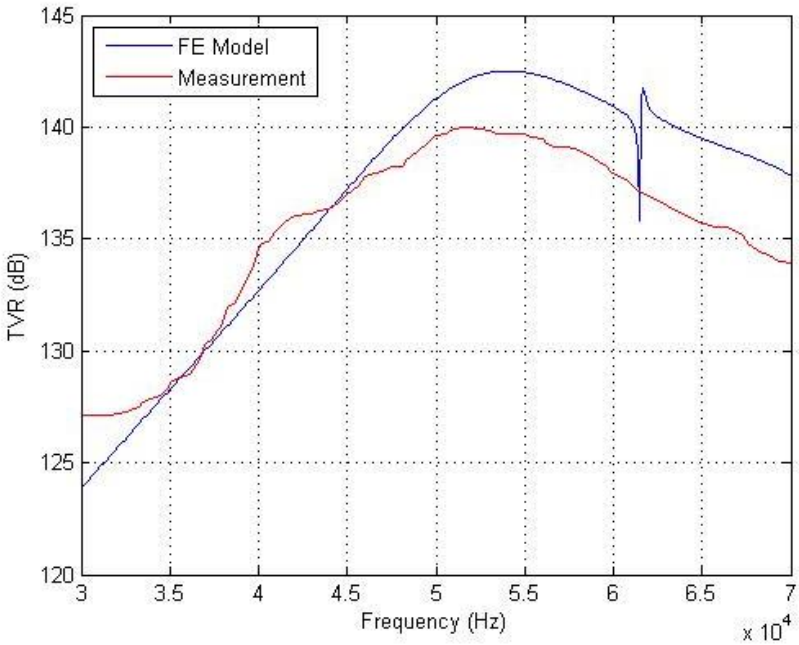

Figure 22: TVRs of FE Model of the Reference Transducer and the Measurement

Table 5: Measurement and the Finite Element Model Results

	Measurement	Simulation	Relative Error [%]
Resonance Frequency (f_n)	50 kHz	50.4 kHz	0.8
TVR	140.06 dB	142.8 dB	1.9

4.4. Comparison of Models

The models introduced in Chapter 3.1 – 3.3 are compared according to in-water conductance and transmitting voltage responses. For better visualization, the in-water conductance (Figure 23) and the TVRs (Figure 24) of all the models and the measurement are shown on the same graph.

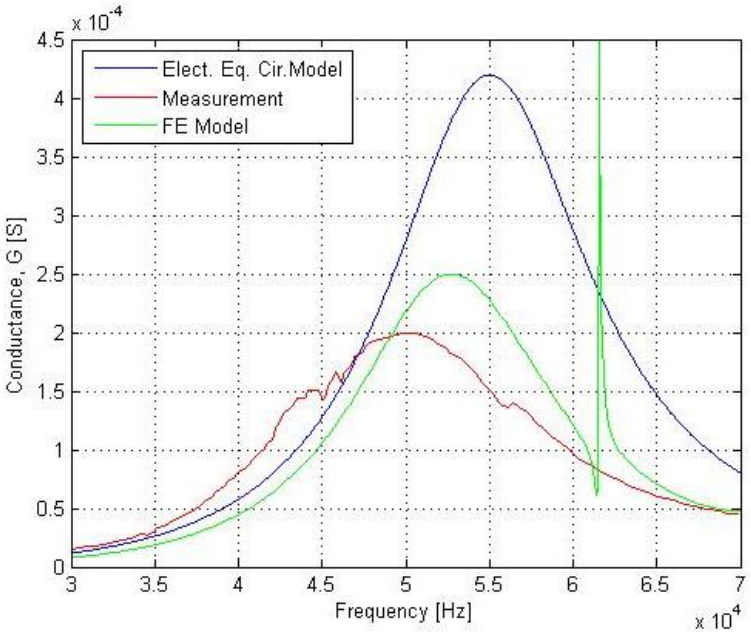

Figure 23: In-water Conductance Responses of Transducer Models and the Measurement

The in-water conductance result is considered mainly for determining the resonance frequency of the transducer. The results are in good agreement with the expectations as far as the resonance frequencies of the corresponding models are concerned. The accuracy of estimated resonance frequency of the model increases as the detail of the model increases as expected. During modeling process, no efficiency term is taken into consideration; therefore, it is also expected that the conductance values of models are 2 or 3 times of the actual value. In addition, the peak conductance value regarding to Electrical Equivalent Circuit Model is higher than the value of FE Model as the head mass is assumed to have a uniform velocity in Electrical Equivalent Circuit Model with no resistive terms. However, for FE model, uniform vibration velocity assumption is not valid. Therefore, the peak conductance value is closer to the measurement value.

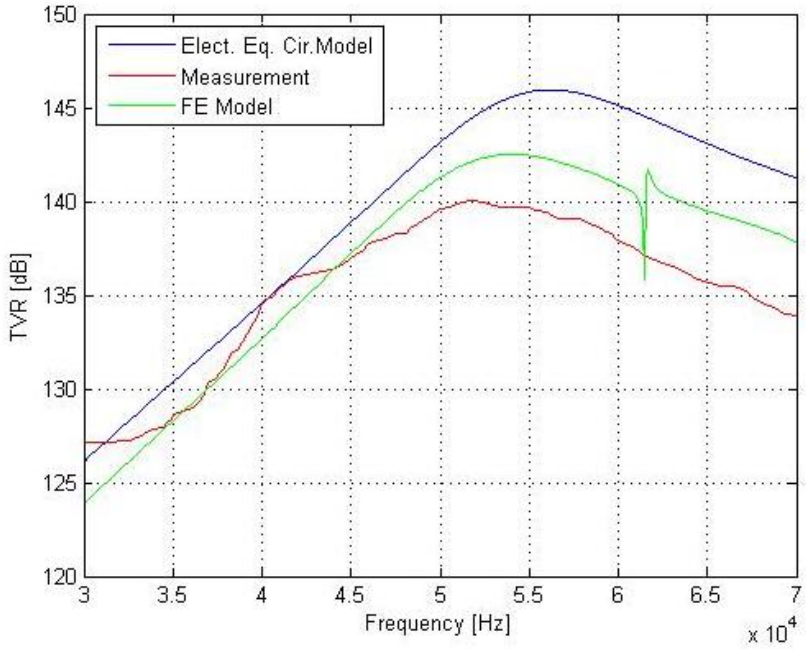

Figure 24: TVRs of Transducer Models and the Measurement

All models have higher TVR values than the measurement since models have ideal conditions with no losses. In other words, during modeling processes, it is assumed that the efficiencies of the transducer are unity. On the other hand, the actual efficiency of reference 50-kHz transducer is declared as 63% in Bayliss' PhD dissertation. The difference between peak values of FE model and the measurement is around 2 dB which corresponds to the discrepancy of efficiencies of FE model and the measurement. Therefore, FE model can be accepted as to give reasonably accurate results very useful in transducer designing. However, when the computation time is considered, FE model needs more processing times than other models.

Table 6: Results and regarding Relative Errors for Transducer Models

	Resonance Frequency	Relative Error
Simple Lumped Parameter Model	64.2 kHz	28.4 %
Electrical Equivalent Circuit Model	55 kHz	10 %
FE Model	50.4	0.8 %

CHAPTER 5

OPTIMIZATION

In this part, optimization of design parameters for Tonpilz-type transducers is conducted. First, the design requirements of the transducer should be defined. The goal of this problem is to design a pinger transducer with resonance frequency of 15 kHz. Pinger transducers need to emit sound signal in one tone and directional properties of the transducer is not so important. However, the level of the emitted sound signal should be as high as possible. Therefore, bandwidth and beam width of the transducer is not considered; however, the output power, in other words, TVR is maximized.

There are three design models for transducers introduced in Chapter 3. Electrical Equivalent Circuit Model and Finite Element Model give transducer performance metrics (resonance frequency and TVR) when the transducer design parameters, such as dimensions, are inputs. However, Simple Lumped Parameter Model gives the design parameters (mass of the head mass, mass of the tail mass and dimensions of piezoceramic stack) when the desired transducer performance metrics are identified. Therefore, an optimization algorithm could be implemented to Electrical Equivalent Circuit Model and Finite Element Model. The initial design parameters for optimization algorithms could be obtained with the help of Simple Lumped Parameter Model discussed in Chapter 3.1. Optimization with Electrical Equivalent Circuit Model can only be possible for lumped parameters. However, FEM allows optimization of not only lumped parameters but also the dimensions of the transducer. Therefore, two optimization processes are conducted with FEM.

The introduced transducer models are complicated functions and not differentiable; thus, traditional optimization algorithms would not be capable of finding the optimum value. Non-traditional optimization algorithms such as non-linear goal programming and genetic algorithm have to be used in optimization process. In this study, genetic algorithm is used for the optimization of transducer models.

5.1. Obtaining Initial Design Parameters

Among all the models explained in Chapter 3, the only model which can give initial design parameters of the transducer is the Simple Lumped Parameter Model. The process begins with the determination of the radius of the active surface. As mentioned before, the radius of the active surface is settled utilizing the assumption of uniform oscillation velocity for the head mass. Furthermore, head mass is assumed to be running in a rigid baffle. The radius of the head mass could be decided based on the maximum value for radiation resistance shown in A.1. The process of solving the equations in Chapter 1 begins with the determination of quality factor, Q_m, of the transducer. Therefore, bandwidth of the transducer should be fixed. At this stage, the bandwidth of the transducer is fixed as 5000 Hz.

With knowing the active surface radius and the mechanical quality factor from design requirements and equation 3.10; other dimensions of the transducer could be obtained easily with the design assumption such as tail-to-head mass ratio introduced in Equation 3.13. The next step is to check flexural resonance of the head mass. The flexural resonance is desired to be at least 2 times of the resonance frequency of the transducer to avoid flapping motion of the head mass.

A Matlab code is generated to solve set of equations introduced in section 3.1. The procedure begins with the determination of the *mechanical quality factor, Q_m*. To find the quality factor, resonance frequency and the bandwidth should be known. The aim is to design a pinger transducer with a resonance frequency of 15 kHz. Therefore, the resonance frequency is comprehended while there is no specification

for the bandwidth of the transducer. The bandwidth of the transducer is decided to be 5000 Hz for the calculations. The design parameters after the calculations are presented in Table 7.

Table 7: Lumped Transducer Parameters According to Simple Lumped Parameter Model

M_h [kg]	r_h [mm]	M_t [kg]	r_{pzt_out} [mm]	r_{pzt_in} [mm]	t_{pzt} [mm]
0.363	41.4	1.454	23.1	13.9	7.4

To examine the initial parameters represented in Table 7 with FEM, some geometrical assumptions are made which can be observed from Figure 25. The head mass is assumed to have a cylindrical and a conical part with same height. The radius of the cylindrical part of the transducer is equal to the active surface radius and determined with Simple Lumped Parameter Model. The smaller radius of the conical part is taken a value between outer radius of the piezoceramic stack and the active surface radius. Inner radius of the tail mass is decided to be 1 mm greater than the radius of the stud. The results regarding to FEM of this transducer geometry with initial parameters are represented in Figure 26 and Figure 27.

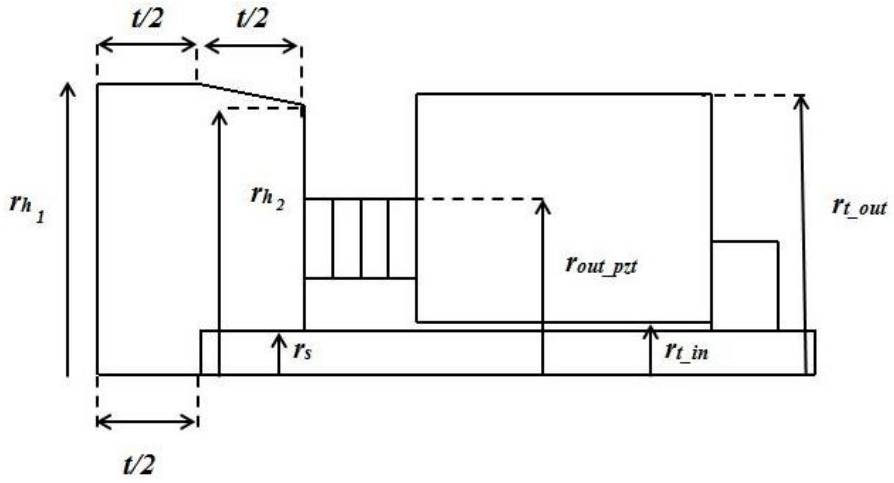

Figure 25: Assumed Transducer Geometry

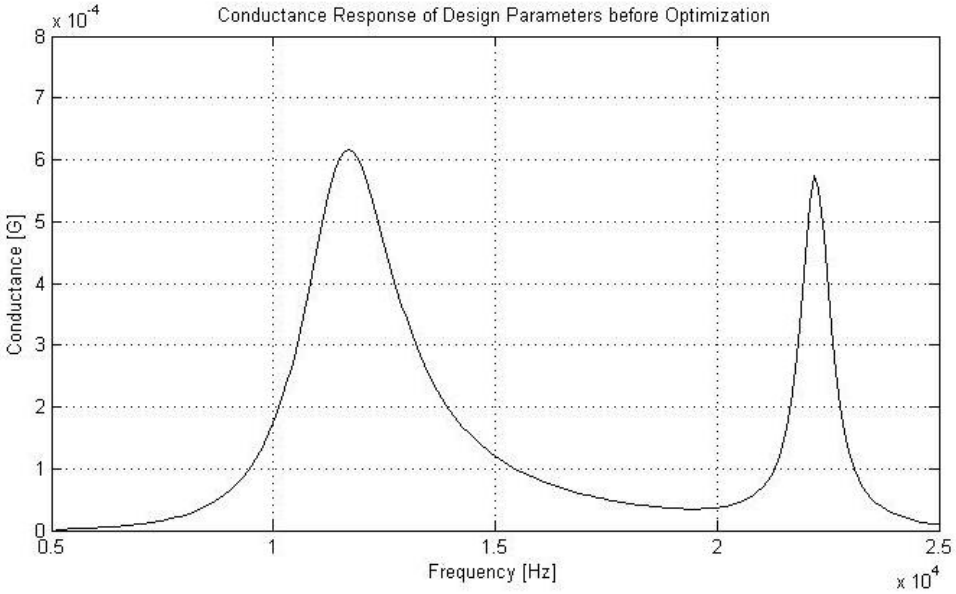

Figure 26: FEM Conductance Response of Initial Design Parameters

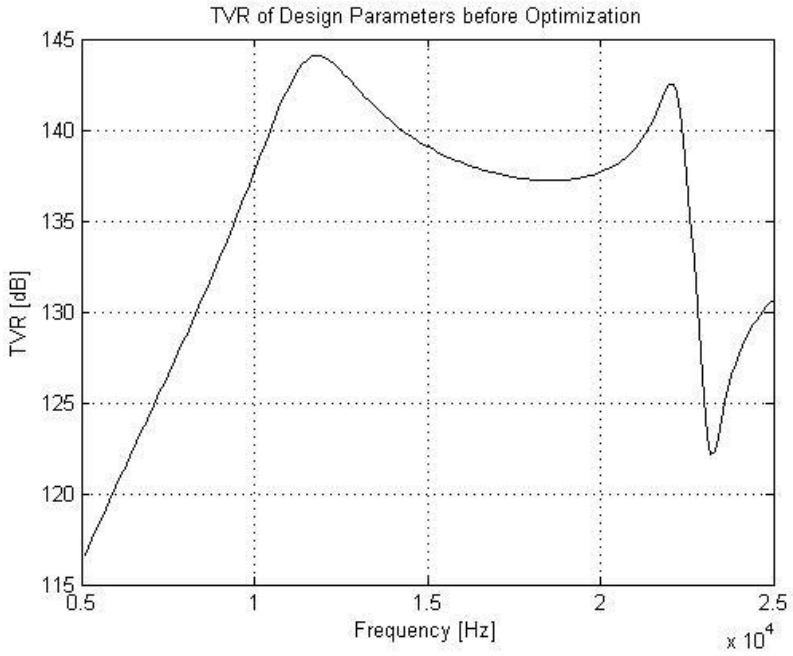

Figure 27: FEM TVR of Initial Design Parameters

5.2. Optimization of Design Parameters with Electrical Equivalent Circuit Method

Optimization Toolbox of MATLAB is used to optimize the initial design parameters in Chapter 5.1.; Optimization process begins with the choice of design variables. Six variables are used for optimization. These are radius of the active surface, mass of the head mass, mass of the tail mass, outer radius of piezoceramics, inner radius of piezoceramics and thickness of a ceramic.

The next step is the formulation of constraints. Three constraints are defined for the problem:

$$r_{pzt\_out} \leq r_h$$

$$2M_h \leq M_t$$

$$r_{pzt\_in} \leq r_{pzt\_out}$$

To complete the optimization problem construction, upper and lower bounds for variables have to be decided. The problem does not require any lower bound. For dimensional design variables such as radius of the active surface, *λ/4* is taken as an upper bound. Also, since practically piezoceramic thickness greater than 10 mm is not useful, for thickness of piezoceramics, 10 mm is taken as an upper bound.

As mentioned before, genetic algorithm is used for the optimization. Population type is "Double Vector" and for the selection of individuals "Tournament" is used. Figure 28 shows the Optimization Toolbox with the explained settings.

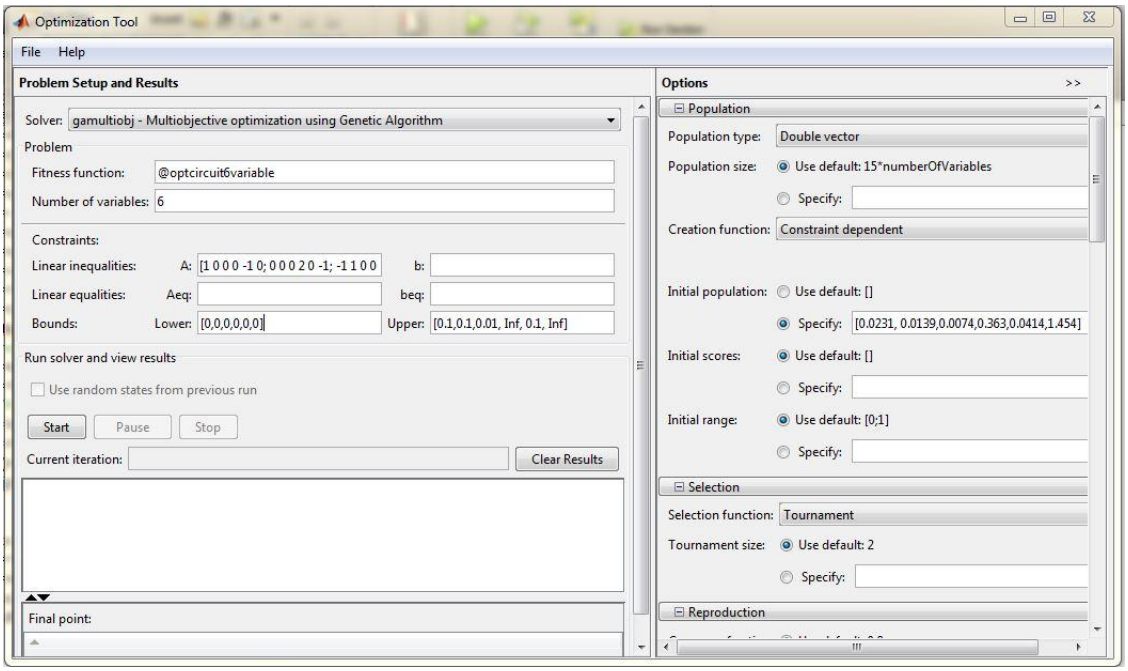

Figure 28: A representative figure of MATLAB Optimization Toolbox

Table 8: Design Parameters before and after the Optimization with Electrical Equivalent Circuit Model

	M_h [kg]	r_h [mm]	M_t [kg]	r_{pzt_out} [mm]	r_{pzt_in} [mm]	t_{pzt} [mm]
Before Optimization	0.363	41.4	1.457	23.1	13.9	7.4
After Optimization	0.404	66.9	1.478	26.5	9.2	3.9

The results are examined with FEM according to the geometry presented in Figure 25. The conductance response and the TVR can be observed from Figure 29 and Figure 30.

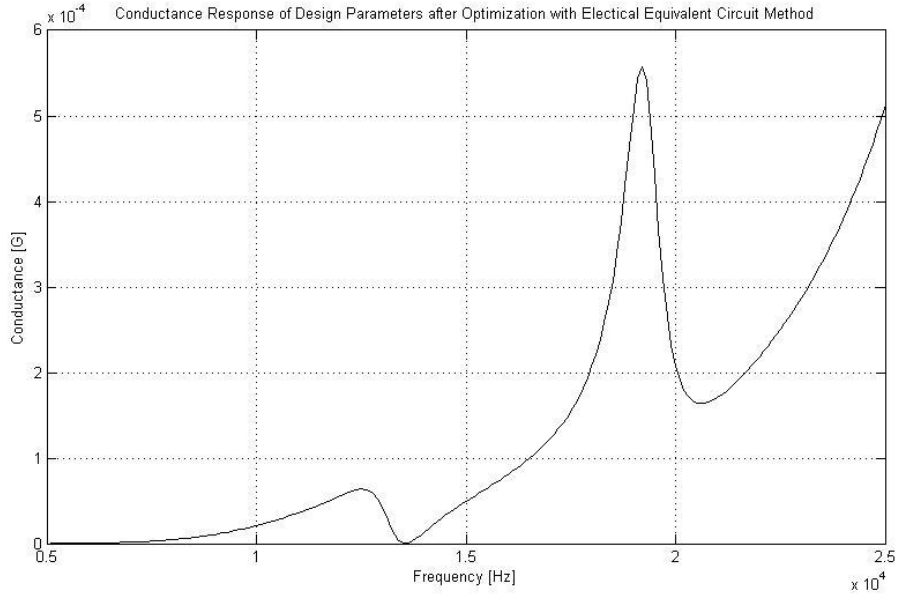

Figure 29: Conductance Response of Design Parameters Optimized with Electrical Equivalent Circuit Model

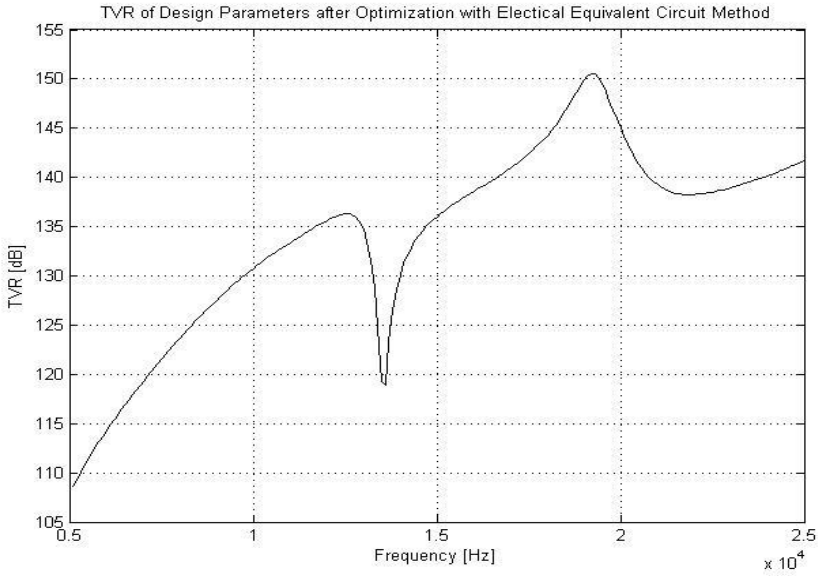

Figure 30: TVR of Design Parameters Optimized with Electrical Equivalent Circuit Model

5.3. Optimization of Lumped Design Parameters with Finite Element Method

In this part, the initial parameters in Chapter 5.1 are optimized with Finite Element Method. As the lumped parameters cannot be optimized with FEM, the parameters are converted into dimensional parameters. The same method used for analyzing the initial parameters with FEM is utilized for this purpose.

The optimization is conducted with the same settings of Chapter 5.2. Design parameters after optimization could be observed from Table 9.

Table 9: Lumped Design Parameters before and after the Optimization with FEM

	M_h [kg]	r_h [mm]	M_t [kg]	r_{pzt_out} [mm]	r_{pzt_in} [mm]	t_{pzt} [mm]
Before Optimization	0.363	41.4	1.457	23.1	13.9	7.4
After Optimization	0.367	38.7	1.12	26.2	14	7.1

The FEM conductance response and TVR regarding to the parameters presented above could be seen from Figure 31 and Figure 32, respectively.

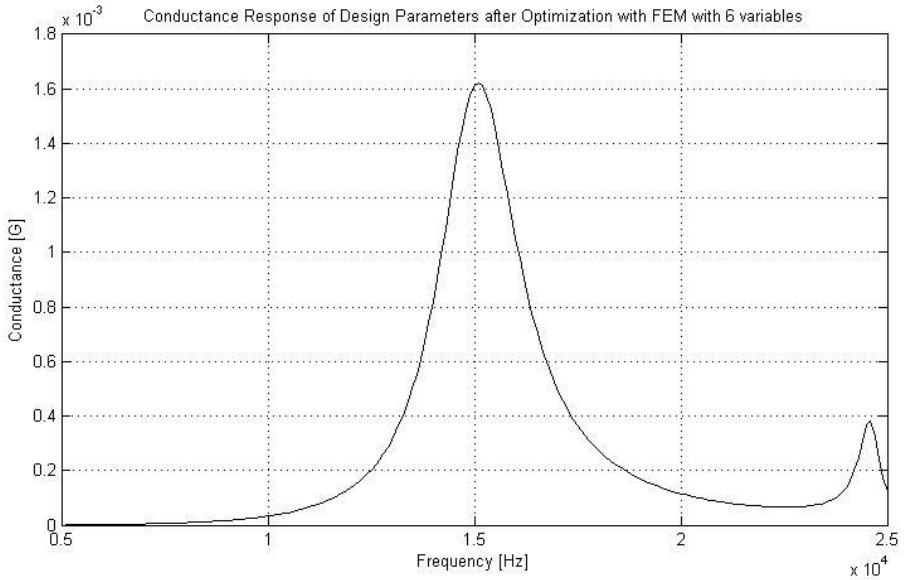

Figure 31: Conductance Response of Lumped Design Parameters Optimized FEM

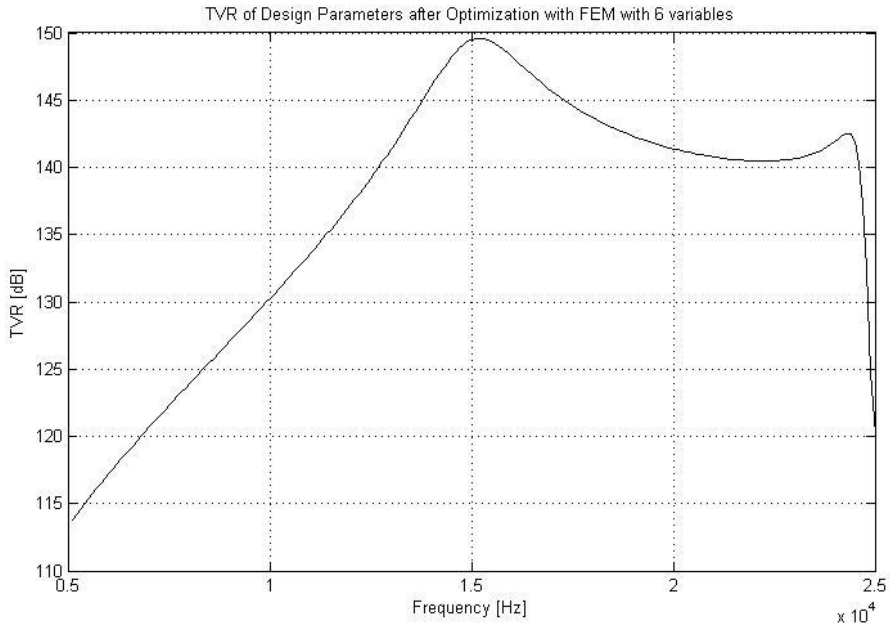

Figure 32: TVR of Lumped Design Parameters Optimized FEM

5.4. Optimization of Dimensional Parameters with Finite Element Method

In this section, the dimensions of the transducer are optimized with genetic algorithm. To decide the dimensional parameter that are going to be optimized, first a general shape for Tonpilz transducer should be settled. Then, according to the shape, dimensions of the transducer are chosen. The assumed transducer shape and the dimensional properties determined to be optimized are presented in Figure 33 below. Not all the dimensions are included in the optimization process; instead, some dimensional parameters are assumed to take a value which parametrically changes according to another value. For instance, inner diameter of the tail mass is settled to be 1 mm greater than the radius of the stud. In addition, the length of the stud is decided according to the lengths of the tail mass, head mass, nut and the piezoceramic stack.

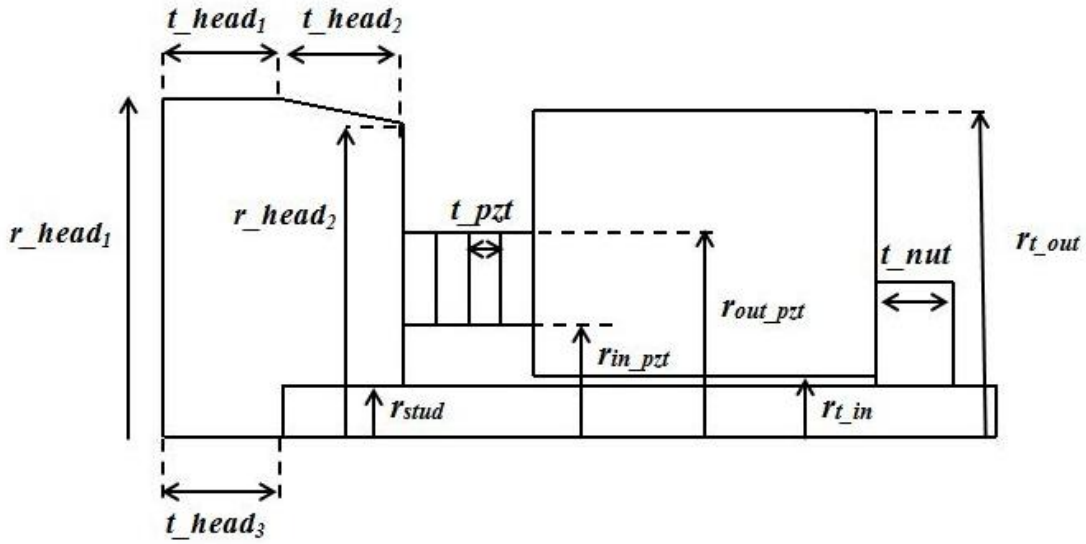

Figure 33: An Introductory Sketch of Dimensional Parameters of Tonpilz Transducer

The initial dimensional parameters are achieved via the method explained in Chapter 5.1. The initial and the final dimensional parameters could be seen from Table 10.

Table 10: Dimensional Design Parameters before and after the Optimization with FEM in mm

	r_{out_pzt}	r_{in_pzt}	t_{pzt}	r_{head1}	r_{head2}	t_{head1}	t_{head2}	t_{head3}	r_{stud}	t_{nut}	r_{out_tail}	t_{tail}
Before Optimization	23.1	13.9	7.4	41.4	34.7	13.3	13.3	13.3	6	9	38	43
After Optimization	27.4	13.4	6.7	41.3	37.2	14.1	16.2	14.7	10.3	8.8	38	46

The conductance response and TVR regarding to the dimensions given in Table 10 are presented in Figure 34 and Figure 35, respectively.

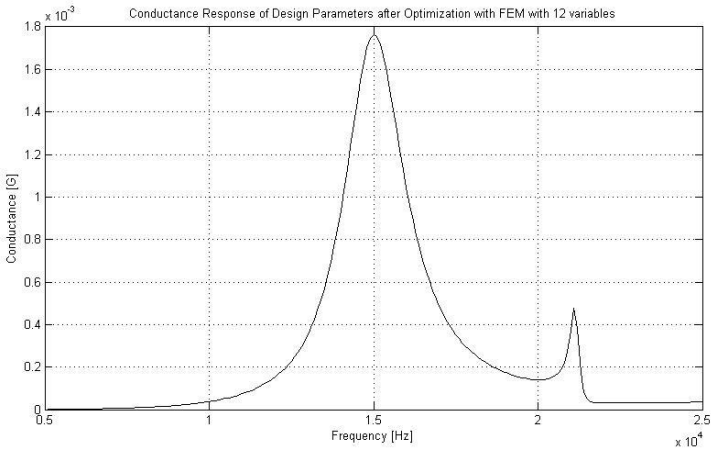

Figure 34: Conductance Response regarding to Optimized Dimensions of Tonpilz Transducer

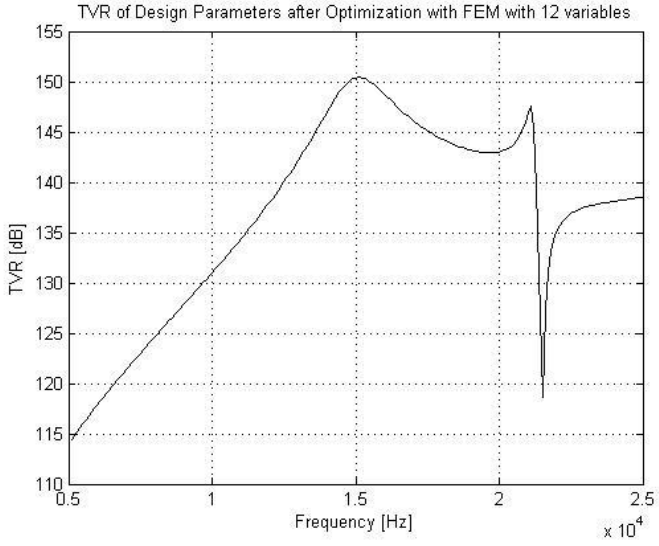

Figure 35: TVR of Tonpilz Transducer with Optimized Dimensions

CHAPTER 6

CONCLUSIONS

In this study, optimization of design parameters for Tonpilz type transducers is conducted. Before optimization of design parameters, all of three models used in the study are introduced. Then, all the models explained in Chapter 3 are validated by utilizing the Tonpilz transducer introduced in Bayliss' PhD dissertation. Also, a conductance study is conducted for FEM.

The lumped parameter model is used not for optimization but for establishment of initial design parameters. With application of the first model, lumped parameters are obtained. When these parameters are analyzed in the second model, namely, the electrical equivalent circuit model, it is obviously seen that the design parameters are not sufficient for the design requirements. Thus, an optimization algorithm needs to be employed to improve the design parameters. The parameter set obtained after optimization, both enhances the frequency and TVR responses. However, when FE models are used, it has become apparent that the resonance frequency of the parameter set is not convenient (Figure 29 and Figure 30). This may because both the lack of accuracy of the electrical equivalent circuit model and the geometrical assumptions made for FE modeling. Therefore, a model including geometrical properties is necessary for a more reliable optimization.

FE method proves to be the most reliable method among all the modeling methods introduces. Hence, FE model is used for optimization. First, lumped parameters obtained via Simple Lumped Parameter Model are optimized with FE model. In order to optimize lumped parameters such as mass of the head mass, the lumped parameters have to be turned into dimensional parameters. For achieving this goal, a

transducer model with certain assumptions such as head mass which consists of a cylindrical and a conical halves is formed. The conductance response and the TVR of the optimized case can be observed from Figure 31 and Figure 32, respectively.

Lastly, dimensions of a Tonpilz transducer are optimized. To compare the results with the previous optimization, the same transducer geometry is assumed (Figure 25). The head mass is decided to have a cylindrical and a conical part. Also, the head mass is just a simple cylinder with a hole. In this process, some dimensions of the transducer are parametrically assumed in terms of other dimensions. For instance, the inner radius of the tail mass is not included in optimization; it is basically accepted as 1 mm larger than the radius of the stud. In addition, the length of the stud is found from the lengths of the piezoceramic stack, tail mass and nut. Other twelve dimensions are integrated into the optimization process. The conductance response (Figure 34) and TVR (Figure 35) of the optimized dimensions are illustrated below.

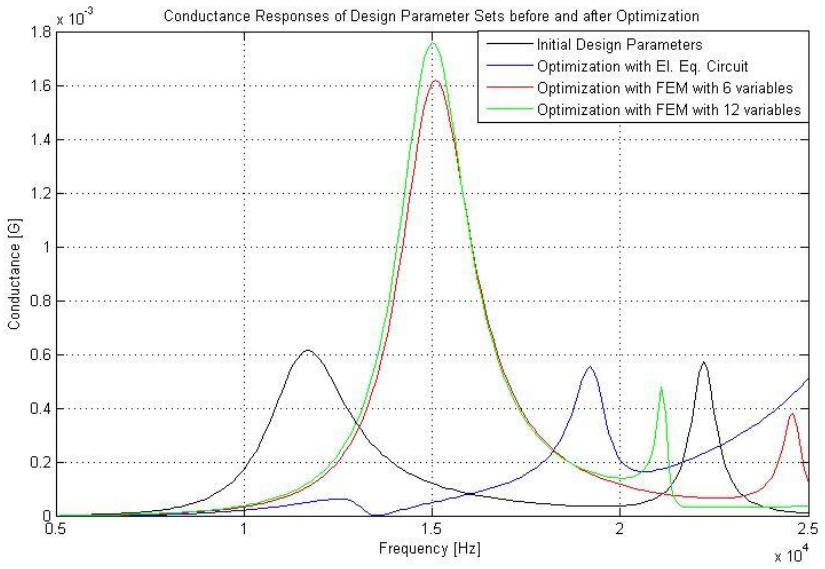

Figure 36: Comparison of Conductance Responses of Parameter Sets

Conductance responses of all parameter sets can be seen from Figure 36. As obvious from the figure, initial design parameter set and the parameter set optimized with Electrical Equivalent Circuit Model do not satisfy the resonance frequency requirement. Although, optimizing with Electrical Equivalent Circuit Model enhances the conductance response; the maximum conductance frequency which implies the resonance frequency is still far from the desired value. On the other hand, when the optimization results of finite element model are examined, it is obviously seen that the both lumped parameter optimization and dimension optimization yield the requested resonance frequency almost exactly.

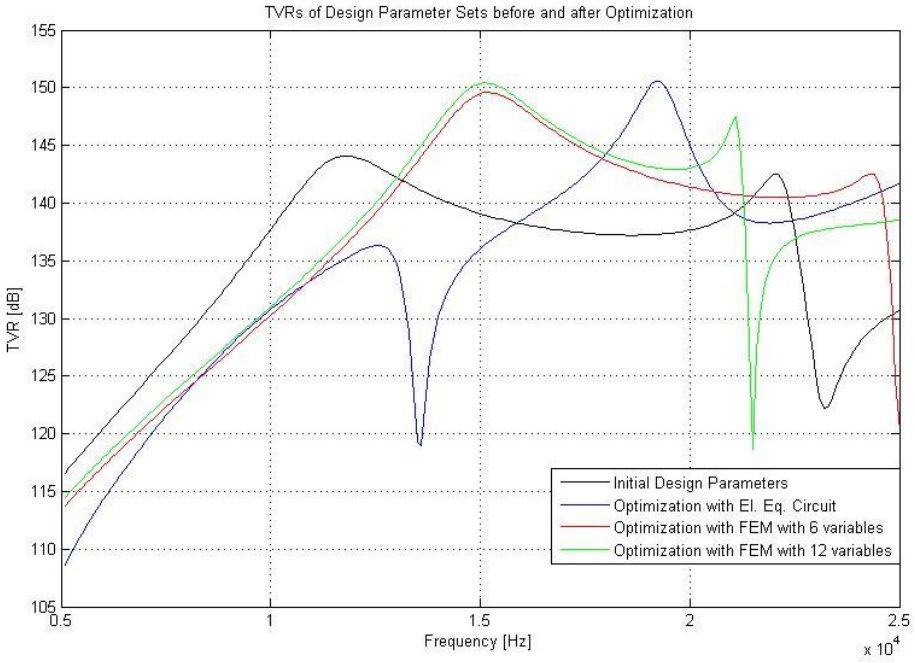

Figure 37: Comparison of TVRs of Parameter Sets

Transmitting Voltage Responses regarding to the design parameters have the same behavior with the conductance responses. Surprisingly, optimization with Electrical Equivalent Circuit Model also gives acceptable TVR values. However, since the

frequency where TVR of nearly 151 dB occurs is not the resonance frequency. When the TVR at the resonance frequency is taken into consideration, not much improvement is observed. In addition, optimization of dimensional parameters with FEM presents a slightly better solution according to TVR.

In conclusion, the purpose of this study is to optimize design parameters of Tonpilz type transducers. Three optimization alternatives are conducted during the study. One is optimization of initially obtained lumped design parameters via Electrical Equivalent Circuit Model. Then, another optimization is carried on to investigate the results of optimization of lumped parameters with Finite Element Model. Last, the most comprehensive optimization study is performed which is optimization of a transducer's dimensions with FEM.

All the results obtained indicate that optimization with Electrical Equivalent Circuit Model does not reveal sufficient results. Main reason for this can be attributed to the inaccuracy of the model. Although the optimization reaches an optimum value according to Electrical Equivalent Circuit Model, the result may not be satisfactory when analyzed by means of a more accurate model. On the other hand, optimization with Finite Element Model yields sufficiently accurate results. In this study, two different optimizations are conducted utilizing FEM. One is the optimization of lumped parameters. The other is the dimensional optimization. It is obviously seen that results of both optimization are very close to each other.

The scope of this thesis is to design a pinger transducer with a resonance frequency of 15 kHz. Therefore, the aim of the optimization is to maximize the TVR of the transducer at the desired frequency. The other performance characteristics such as bandwidth and beam width are not involved. Further study of this issue would be of interest; since many transducers have design requirements on these parameters. In addition, in this study, discrete parameters of the transducer are taken constant and not optimized. For example, in the problem analyzed the number of ceramics in the piezoceramic stack is taken constant. A future work will involve a optimization which could contain such discrete parameters. Besides, this study only offers a

solution with constant materials. However, a solution with more material options for all transducer parts would be more beneficial for designers. Last, a system which proposes more than one solution for a transducer design problem could be developed for further study on the subject.

REFERENCES

[1] History of Underwater Acoustics, Last accessed by May 14, 2014, http://www.dosits.org/people/history/pre1800/

[2] Urick, R. J., 1983, *Principles of Underwater Acoustics*, Peninsula Publishing, Los Altos, California

[3] Lasky, M., "Review of Undersea Acoustics to 1950," Journal of the Acoustical Society of America, 61(2), pp 283-297

[4] Sherman, C. H., Butler, J. L., 2007, *Transducers and Arrays for Underwater Sound*, Springer, New York

[5] Hunt, F. V., 1954, *Electroacoustics*, John Wiley and Sons, New York

[6] D'Amico, A., Pittenger, R., 2009, "A Brief History of Active Sonar," Aquatic Mammals, 35(4), pp 426-434

[7] Burdic, W.S., 1984, *Underwater Acoustic System Analysis*, Prentice-Hall, New Jersey

[8] Stansfield, D., 1991, *Underwater Electroacoustic Transducers*, Peninsula Publishing, California

[9] Çepni, K., 2011," A Methodology for Designing Tonpilz-Type Transducers", MSc Thesis, Middle East Technical University, Ankara, Türkiye

[10] Cochran, J. C., 2014, *Elements of Sonar Transducer Design*, Applied Technology Institute (ATI) Course Notes, March 2013

[11] Kholkin, A. L., Pertsev, N. A., Goltsev, A. V., 2008, "Piezoelectricity and Crystal Symmetry", ed. By Safari A. and Akdoğan E. K., *Piezoelectric and Acoustic Materials for Transducer Applications*, Chapter 2, Springer.

[12] Fu, B. Hemsel, T., Wallasscheck, J. "Piezoelectric transducer design via multiobjective optimization," Ultrasonics, vol 44, 2006, pp 747-752

[13] McCammon, D. F., Thompson, W., 1980, "The Design of Tonpilz Piezoelectric Transducers using Nonlinear Goal Programming", Journal of the Acoustical Society of America, 68(3), pp 754- 757

[14] Meirowitch, L., 2001, *Fundamentals of vibrations*, McGraw Hill, Boston

[15] Feng, F., Shen, J., Deng, J., 2006, "A 2D equivalent circuit of piezoelectric ceramic ring for transducer design", Ultrasonics, 44, p. e723-e726

[16] Mason, W. P., 1938, *Electromechanical Transducers and Wave Filters*, Van Nostrand, New York

[17] Krimholtz, R., Leedom, D. A., Matthaei, G. L. 1970, "New equivalent circuits for elementary piezoelectric transducers", Electronic Letters, 6(13), pp. 398-399

[18] Chubachi, N., Kamata, H., 1996, "Various equivalent circuits for thickness mode piezoelectric transducers", Electronics and Communications in Japan, Part 2, 79(6), pp. 50-59

[19] Tilman, H. A. C., 1996, "Equivalent circuit representation of electromechanical transducers: I. Lumped parameter systems", Journal of Micromechanics and Microengineering, 6, pp. 157-176

[20] Ramesh, R., Ebenezer, D. D., 2008, “Equivalent circuit for broadband underwater transducers”, IEEE Transactions on Ultrasonics, Ferroelectrics, and Frequency Control, 55(9)

[21] Aoyagi, T., Koyama, K., Nakamura, K., Tabaru, M., 2010, “Equivalent Circuit Analysis and Design of Multilayered Polyurea Ultrasonic Transducers”, Japanese Journal of Applied Phsysics, 49, p. 07HD05 1-4

[22] Feng, F., Shen, J., Deng, J., 2006, “A 2D equivalent circuit of piezoelectric ceramic ring for transducer design”, Ultrasonics, 44, p. e723-e726

[23] Sherrit, S., Wiederick, H. D., Mukherjee, B. K., Sayer, M., “An accurate equivalent circuit for the unloaded piezoelectric vibrator in the thickness mode”, Journal of Physics D: Applied Physics, 30(16), pp. 2354-2363

[24] Iula, A., Lamberti, N., Pappalardo, M., 1996, “ A model for the theoretical characterization of thin piezoceramic rings”, IEEE Transactions on Ultrasonics, Ferroelectrics, and Frequency Control, 43(3), pp. 370-375

[25] Bjorno, L., 2002, “”Features of Underwater Acoustics from Aristotle to Our Time”, Acoustical Physics, 49(1), pp. 24-30

[26] Iula, A., Lamberti, N., Pappalardo, M., 1998, “An approximated 3-D model of cylinder-shaped piezoceramic elements for transducer design”, IEEE Transactions on Ultrasonics, Ferroelectrics, and Frequency Control, 45(4), pp. 1056-1064

[27] Iula, A., Carotenuto, R., Lamberti, N., Pappallardo, M., 2002, “An approximated 3-D model of the Langevin transducer and its experimental validation”, J. Acoust. Soc. Am., 111(6)

[28] Mančić, D. D., and Stančič, G. Z., 2002, "Piezoceramic ring loaded on each face: a three dimensional approach", Electronic Journal Technical Acoustics, 2, 1.1-1.7

[29] Mančić, D. D., and Stančič, G. Z., 2010, "New Three-dimensional Matrix Models of the Ultrasonic Sandwich Transducers," Journal of Sandwich Structures and Materials, 12(1), pp. 63-80

[30] Vadde, V., Lakshimi, B., 2011, Characterization and FEM-based performance analysis of a Tonpilz transducer for underwater acoustic signaling applications", COMSOL Conference,

[31] Jalihal, P., Vishveshar, S., Prasad, A. M., "Finite element analysis of a Tonpilz Transducer", Advances in Structural Dynamics, pp. 31-37

[32] Hawkins, D. W., Gough, P. T., 1996, "Multiresonance design of a Tonpilz transducer using the finite element method", IEEE Transactions on Ultrasonics, Ferroelectrics and Frequency Control, 43(5), pp. 782-790

[33] Pei, D. L., Roh, Y., 2008. "Design of an underwater Tonpilz transducer with 1-3 piezocomposite materials", Japanese Journal of Applied Physics, 47(5), pp. 4003-4006

[34] Yao, Q., Bjorno, L., 1997, "Broadband Tonpilz underwater acoustic transducers based on multimode optimization", IEEE Transactions on Ultrasonics, Ferroelectrics and Frequency Control, 44(5), pp. 1060-1066

[35] Decarpigny, J. N., Debus, J. C., Tocquet, B., Boucher, D.,1985, "In-air analysis of piezoelectric Tonpilz Transducer in a wide frequency band using a mixed finite element-plane wave method", J. Acoust. Soc. Am., 78(5), pp. 1499-1507

[36] Desilets, C., Wojcik, G., Nikodym, L., Mesterton, K., 1999, "Analyses and measrurements of acoustically matched, air-coupled Tonpilz transducer", IEEE Ultrasonics, 2, pp. 1045-1048

[37] Allik, H., Webman, K. M., Hunt, J. T., 1974, "Vibrational response of sonar transducers using piezoelectric finite elements", J. Acoust. Soc. Am., 56(6), pp. 1782-1791

[38] Smith, B. V., 1994, "The modeling of underwater, electroacoustic, sonar transducers", Applied Acoustics, 41, pp. 337-363

[39] Coates, R., 1990, "Modeling acoustic transducers: problems and some possible solutions", OCEANS'90 Engineering in the Ocean Environment Conference Proceedings, pp. 544-549

[40] Teng, D., Chen, H., Zhu, N., Zhu, G. and Gou, Y., 2008, " Comparison of Design Methods of Tonpilz Type Transducers", Global Design to Gain a Competitive Edge, Springer, pp. 81-89

[41] Silva, E: C. N., Kikuchi, N., 1999, "Design of Piezoelectric Transducers Using Topology Optimization", Smart Materials and Structures, 8(3), pp. 350-364

[42] Saijyou, K., Okuyama, T., 2010, "Design Optimizaiton of Wideband Tonpilz Piezoelectric Transducer with a Bending Piezoelectric Disk on the Radiation

Surface", J. Acoust. Soc. Am., 127[5], pp.2836-2846

[43] Kai, Z:, De-shi, W., 2011, "Study on Optimization Parameters to Tonpilz Transducers", Computing Control and Industrial (CCIE) 2011 IEEE 2nd International Conference on, 2, pp. 414-416

[44] Reynolds, P., Pereyra, V., 2004, "Application of Optimisation Techniques to Finite Element Analysis of Piezocomposite Devices", IEEE International Ultrasonics, Ferroelectrics and Frequency Control, pp. 634-637

[45] Van Crombrugge, M., Thomson, W., "Optimization of the transmitting characteristics of a Tonpilz type transducers by proper choice of impedance matching layers",

[46] Deb, K., 1995, *Optimization for Engineering Design Algorithms and Examples*, PHI, New Delhi

[47] Houck, C. R., Joines, J. A., Kay, M. G., "A Genetic Algorithm Function Optimization: A Matlab Implementation"

[48] Goldberg, D., 1989, *Genetic Algorithms in Search, Optimization and Machine Learning*, Addison-Wesley

[49] Khan, M. S., Cai, C., Hung, K.C., 2002, "Acoustic field and active structural acoustic control modeling in Ansys", International Ansys Conference,

[50] Kim, J., Kim, H. S., 2009, "Finite Element Analysis of Piezoelectric Underwater Transducers for Acoustic Characteristics", Journal of mechanical Science and Technology, 23, pp. 452-460

[51] Bayliss, C., 1998, " Application and Development of Finite Element

Techniques for Transducer Design and Analysis", PhD Thesis, The University of Birmingham, Birmingham, UK

[52] Dunn, J. R., 1987, "Some Aspects of Transducer Design by Finite Element Modeling Techniques", ed. by Merklinger, H., M., Progress in Underwater Acoustics, p. 639- 645, Plenum Press.

[53] Castillo, M., Acevedo, P., Moreno, E., 2003, "KLM model for lossy piezoelectric transducers", Ultrasonics, 41, pp. 671-679

APPENDIX A

BRIEF INFORMATION ABOUT RADIATION IMPEDANCE

A.1. Definition of Radiation Impedance

Radiation impedance can be basically defined as the ratio of the force exerted to the acoustic medium from vibrating surface to the normal vibration velocity of the surface. Radiation impedance is a mechanical term; however, it has electrical analogous, electrical impedance which is the ratio of the voltage to current. Radiation impedance can also be expressed as a combination of radiation resistance and radiation reactance. The definitions of radiation impedance can be observed as follows:

$$Z_r = \frac{F}{u} \qquad Z_r = R_r + jX_r \tag{A.1}$$

where Z_r is the radiation resistance, F is the force exerted by the vibrating surface, u is the vibration velocity of the surface. Radiation resistance, R_r, as seen from A.1, is the real part of the radiation impedance; while, radiation reactance, X_r, is the imaginary part of the radiation impedance.

Radiation impedance which can be achieved by multiplying pressure and velocity over the active surface is directly related with the near field of the transducer. In addition, radiation resistance is an indicator of the performance of the transducer since it is related with the power transmitted to the acoustic medium. Besides,

radiation reactance affects resonance frequency and bandwidth of the transducer. Due to these reasons, radiation impedance is one of the most important characteristics of the transducers.

A.2. Radiation Impedance of a Circular Piston in a Rigid Baffle

In transducer design process, the goal is to achieve a radiation impedance of circular piston in a rigid baffle. In this section, analytical representation of radiation impedance of circular piston in a rigid baffle is explained.

In order to obtain radiation impedance of circular piston in a rigid baffle, pressure over the infinitesimal contributions of the vibrating surface is integrating over the surface. Then the result is divided to the normal velocity of the surface. For this calculation, the velocity is assumed to be uniform throughout the surface which is not real case. The radiation impedance of a circular piston in a rigid baffle can be expressed as follows [4]:

$$Z_r = \rho c A\left[\left(1-\frac{J_1(2ka)}{ka}\right)+ j\frac{H_1(2ka)}{ka}\right] \qquad k=\frac{2\pi}{\lambda}=\frac{2\pi f}{c} \tag{A.2}$$

where ρ is the density of the acoustic medium, c is the speed of sound in the acoustic medium, k is the wavenumber, a is the radius of the vibrating surface, ka is the Helmholtz number, λ is the wavelength regarding to the acoustic medium and f is the vibration frequency. J_1 is the Bessel function of first kind of order 1 and H_1 is the Struve function of first kind of order 1. The results are normalized to obtain values which are unitless as well as independent of acoustic medium properties and active surface dimensions. The normalized radiation resistance and reactance values are shown in Figure 38 below:

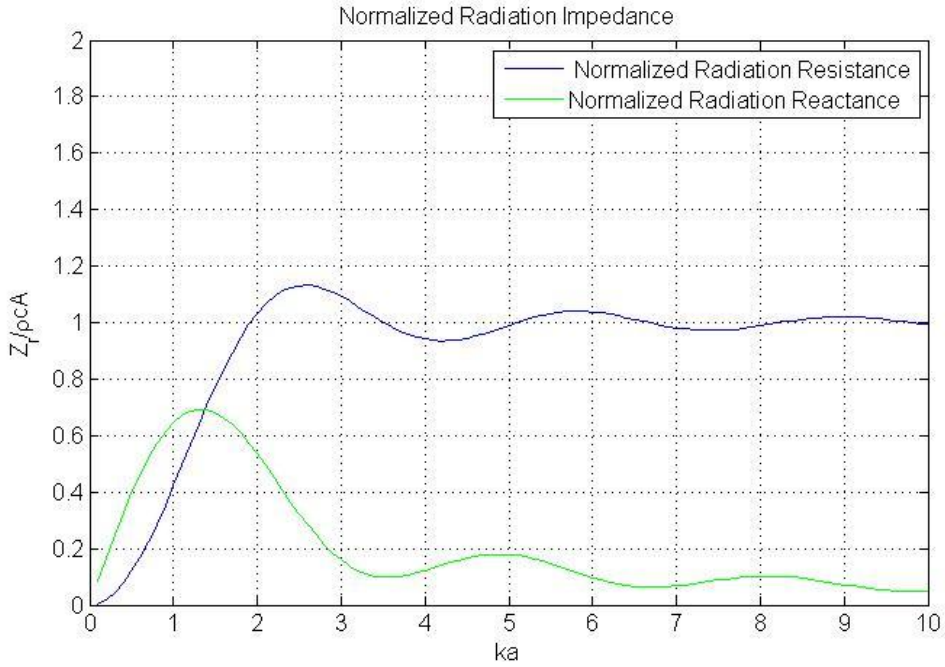

Figure 38: Analytical Results of Normalized Radiation Impedance of Circular Piston in a Rigid Baffle